EFFECT OF STRESS EXPONENT ON STEADY STATE CREEP IN A FUNCTIONALLY GRADED ROTATING DISC

A dissertation report submitted in the partial fulfillment of the requirements for the award of degree of

Master of Engineering

IN

CAD/CAM & ROBOTICS

Submitted by

SHANKAR SINGH

Roll No: 801181024

Under The Guidance of

Mr. KISHORE KHANNA
(Assistant Professor)
Department of Mechanical Engineering,
Thapar University, Patiala.

DEPARTMENT OF MECHANICAL ENGINEERING
THAPAR UNIVERSITY, PATIALA – 147004.

JULY 2013.

DECLARATION

I hereby declare that the dissertation report entitled **"EFFECT OF STRESS EXPONENT ON STEADY STATE CREEP IN A FUNCTIONALLY GRADED ROTATING DISC"** is an authentic record of my study carried out as partial fulfilment for the award of the degree of **Master of Engineering in CAD/CAM & Robotics** at **Thapar University, Patiala** under the guidance of **Mr. Kishore Khanna, Assistant Professor, Department of Mechanical Engineering, Thapar University, Patiala** in **July 2013**. The matter in this report has not been submitted in part or full to any other university or any institution for the award of any other degree.

Shankar Singh.

(Shankar Singh)

Reg. No. 801181024

This is to certify that above declaration made by the student concerned is correct and to the best of my knowledge and belief.

(Kishore Khanna)

(Assistant Professor)
Department of Mechanical Engineering,
Thapar University, Patiala – 147004

Countersigned by:

Dr. Ajay Batish
Professor and Head,
Department of Mechanical Engineering
Thapar University, Patiala.

Dr. S.K. Mohapatra
Sr. Professor &
Dean of Academic Affairs
Thapar University, Patiala.

ACKNOWLEDGEMENT

I would like to express a deep sense of gratitude and thank profusely to my guide **Mr. Kishore Khanna**for his sincere & invaluable guidance, suggestions and attitude, which inspired me to submit dissertation in the present form. His dynamism and diligent enthusiasm have been highly instrumental in keeping my spirits high. His flawless and forthright suggestions blended with an innate intelligent application have crowned my task with success.

I am grateful to **Dr. Ajay Batish, Professor & Head**, **Mr. Sandeep K Sharma and Mr. Anirban Bhattacharya, P.G Coordinator**, **Department of Mechanical Engineering, Thapar University, Patiala** for providing me an opportunity to do my project work on the topic of my interest and for providing the facilities for the completion of my work.

I take pride of myself being son of ideal parents for their everlasting desire, sacrifice, affectionate blessings, and help, without which it would not have been possible for me to complete my studies.

I would like to thank employees of **Mechanical Engineering Department, Thapar University, Patiala** for their everlasting support and helping advices. Above all, I express my indebtedness to the ***almighty*** for all his blessing and kindness.

(Shankar Singh)

Reg No: 801181024

ABSTARCT

The effect of the stress exponent on steady state creep in a functionally graded rotating disc made up of isotropic Aluminium-Silicon Carbide particulate (Al-SiCp) of constant thickness has been investigated. A mathematical formulation of creep performance described by Sherby creep law and a computer code following the formulation for FGM disc has been developed, with different values of true stress exponent n, varying particle content size (P) with changing reinforcement volume mixtures. It is observed that the radial and tangential stresses and strain rates in disc are extensively affected by variable stress exponent, particle content size and reinforcement volume. But, in fact the trend of stresses and strain rates in the FGM disc remains same by changing the value of the parameters discussed above.

TABLE OF CONTENTS

LIST OF FIGURES

CHAPTER 1

INTRODUCTION TO COMPOSITE MATERIALS

A composite material is a material which is consisting of two or more physically or chemically distinct phases, suitably arranged or distributed. A composite material usually has characteristics that are not shown by any of its components in isolation. A composite material is consisting of two phases continuous and distributed. Generally, the continuous phase is referred to as the matrix, while the distributed phase is termed the reinforcement. There are three items that determine the characteristics of a composite, the reinforcement, the matrix, and the interface among them. In composites, the materials are combined in such a way as to enable to make better use of their qualities while minimizing to some extent the effects of their deficiencies. Designer can make use of tougher and lighter materials, with properties that can be tailored to suit particular design requirements and because of the ease with which complex shapes can be manufactured, the whole reconsidering of an established design in terms of composites can often lead to both cheaper and better solutions.

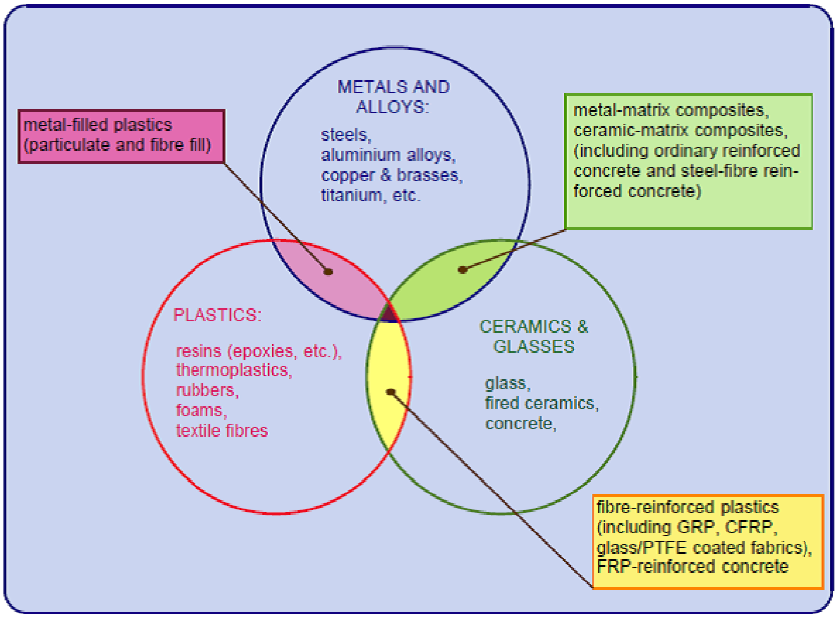

Figure1.1 Relationships between classes of engineering materials [27]

The Figure 1.1 gives a clearer idea of the scope for creativity and relation between different classes of materials which are generally used in engineering design. The structural materials most commonly used in design can be categorized in four primary groups: Metals, Polymers, Composites, and Ceramics. These materials have been used to various degrees since the beginning of time. Figure 1.2 presents a chronological variation of the relative importance of each group.

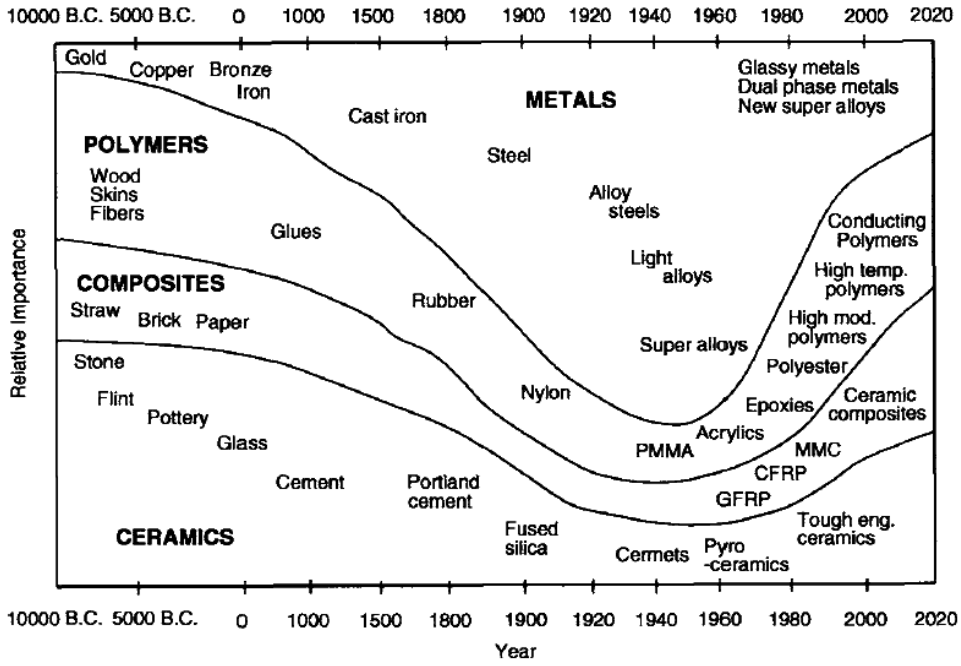

Figure 1.2 Relative importance of material development through history [33]

First, within each group of materials — metallic, ceramic and polymeric — there are already certain familiar materials which can be described as composites. Many members of the mutual and largest group of engineering materials, the family of steels, consist of combinations of particles of hard ceramic compounds in a softer metallic matrix. These particles are sometimes plate-like, sometimes needle-shaped, and sometimes spherical or polygonal. Polymers, too, are often two-phased, consisting of a matrix of one polymer with distributions of harder or softer particles contained within it. As we have seen wood is a perfect example of this. And concrete is a classic example of a ceramic/ceramic composite, with particles of sand and collection of graded sizes in a matrix of hydrated Portland cement. Materials Scientists have learned to control their properties by controlling their microstructures that is to say, the quantity, the form, and the distribution of what it might refer to as the ‘reinforcing phase’. The idea of mixing components across the materials class boundaries is a natural extension of this idea. Making additions of

hard, or fire-resistant, or simply cheap, ceramic powders to plastics to make filled polymers; and making additions of very hard, or abrasive, or thermally stable ceramic particles to metals to make the class of materials known as 'cermets' to produce machine tool tips capable of cutting hard metals at high speeds or high temperatures are only two examples of important developments in our exploitation of these materials. But even more significant is the extension of this principle to incorporate filamentary metals, ceramics and polymers into the bulk forms of any of these three classes of materials to make fibre composites - reinforced plastics, like CFRP and GRP, metal-matrix composites (MMCs) like silicon-carbide-fibre-reinforced aluminium, and ceramic-matrix composites (CMCs) like carbon fibre- reinforced glass.

The composites are generally used in structural applications are best classified as high performance. They are typically prepared from synthetic materials, have high strength-to-weight ratios, and require controlled manufacturing environments for optimum performance.

1.1 CONVENTIONAL MATERIALS AND THEIR LIMITATIONS [27]

There are some of the materials features of metals, plastics and ceramics in order to measure the relative strengths and weaknesses. A comparison in general terms can identify some of the advantages and disadvantages of the different types of material.

1.1.1 PLASTICS are of low density. They have good short-term chemical resistance but they lack thermal stability and have only moderate resistance to environmental degradation. They have poor mechanical properties, but are easily fabricated and joined.

1.1.2 CERAMICS may be of low density. They have great thermal stability and are resistant to most forms of attack (abrasion, wear, corrosion). Although very rigid and strong because of their chemical bonding, they are all brittle and can be formed and shaped only with difficulty.

1.1.3 METALS are mostly of medium to high density, only magnesium, aluminium and eryllium can compete with plastics in this respect. Many have good thermal stability and may be made corrosion resistant by alloying. They have useful mechanical properties and high toughness, and they are moderately easy to shape and join. It is largely a consequence of their ductility and resistance to cracking that metals, as a class, became (and remain) the preferred engineering materials

1.2 COMPOSITE MATERIALS CLASSIFICATIONS [25]

Composite materials are usually classified according to the type of reinforcement used. Two broad classes of composites are fibrous and particulate. Each has unique properties and application potential.

1.2.1 FIBROUS: -A fibrous composite consists of either continuous (long) or chopped (whiskers) fibers suspended in a matrix material. Both continuous fibers and whiskers can be identified from a geometric viewpoint:

1.2.1.1 CONTINUOUS FIBERS

1. Having a very high lengths-to-diameter ratio.
2. Generally stronger and stiffer than bulk material.
3. Fiber diameters generally range between (3-200μm) depending upon the fiber.

1.2.1.2 WHISKERS

1**.** Generally considered to be a short, stubby fiber.

2. Broadly defined as having a length-to-diameter ratio of 5 $<l/d<$ 00.

3. Diameters generally range between (0.02-100 μm).

Composites in which the reinforcements are discontinuous fibers or whiskers can be produced so that the reinforcements have either random or biased orientation. Material systems composed of discontinuous reinforcements are considered single layer composites. Continuous fiber composites can be either single layer or multilayered. The single layer continuous fiber composites can be either unidirectional or woven, and multilayered composites are generally referred to as laminates. The material response of a continuous fiber composite is generally orthotropic.

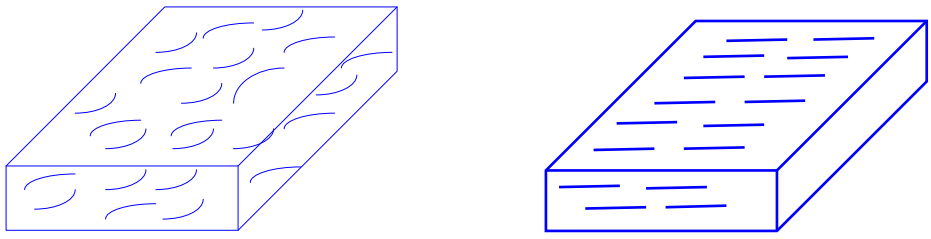

Random Fibre orientation Biased Fibre orientation

Figure 1.3Discontinuous Fibre Composites [33]

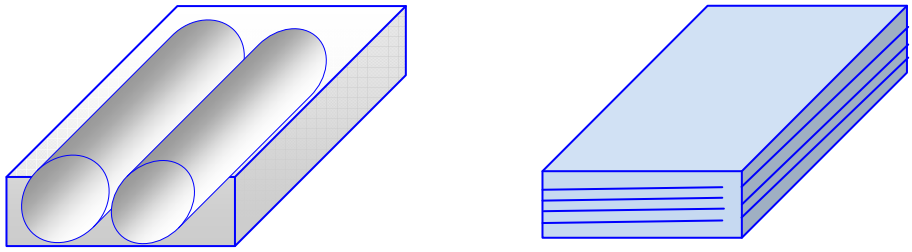

Unidirectional orientation Laminate

Figure 1.4Continuous Fibre Composites [33]

1.2.2 PARTICULATE: - A particulate composite is characterized as being composed of particles suspended in a matrix. Particles can have virtually any shape, size or configuration. Examples of well-known particulate composites are concrete and particle board. There are two subclasses of particulates: Flake and Filled Skeletal

1.2.2.1FLAKE**: -** *Generally* composed of flakes with large ratios of platform area to thickness, suspended in a matrix material (e.g.particle board).

1.2.2.2FILLED/SKELETAL**: -** *Generally* composed of a continuous skeletal matrix filled by a second material: for example, a honeycomb core filled with an insulating material. Such composites are used for many applications in which strength is not a significant component of the design. A schematic of several types of particulate composites is shown in Figure 4.

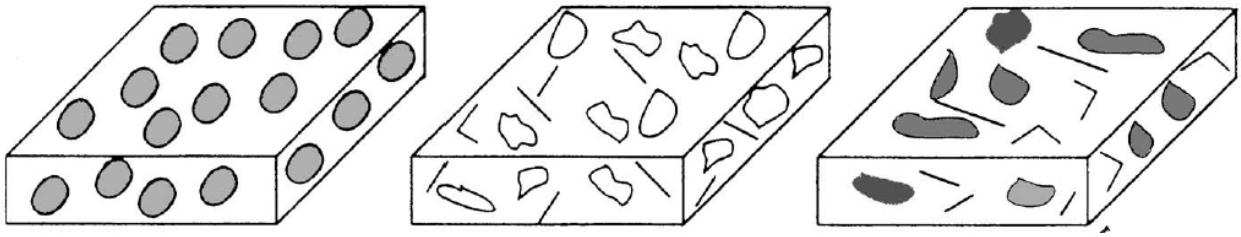

General Particulate Flake Filled/Skeletal

Figure1.5 Schematic representation of particulate composites [33]

1.3 CLASSIFICATION BASED ON MATRIX

Based on the type of matrix, Composites are of the following types [26]

1.3.1 Polymer Matrix Composite (PMC)

1.3.2 Metal Matrix Composite (MMC)

1.3.3 Ceramic Matrix Composite (CMC)

1.3.4 Carbon –Carbon Composite

1.3.1 POLYMER MATRIX COMPOSITE (PMC): Polymer matrix composites are the most advanced composites. These composites consist of a polymer (e.g., epoxy, polyester, urethane etc) reinforced by thin-diameter fibers(e.g., graphite , aramids, boron etc).These are commonly employed due to their low cost, high strength, and simple manufacturing principle. As an example, graphite/ epoxy composites are approximately five times stronger than steel on a weight-for-weight basis. Main drawback of Polymer Matrix Composites (PMCs) include low operating temperature, high coefficient of thermal and moisture expansion and low elastic properties in certain directions. However, the advantages include its strength, low cost, high chemical resistance and good insulating property.

1.3.2 METAL MATRIX COMPOSITE (MMC) This class of composite materials consists of metallic matrix which is usually ductile. The ductile matrix can be aluminum, copper, magnesium, titanium, nickel, super alloy or even an inter-metallic compound. The reinforcing fibers may be graphite, boron carbide, alumina or silicon carbide. Fine whiskers of sapphire, silicon carbide, silicon nitride, wires of titanium, tungsten, molybdenum, beryllium and stainless steel etc have also been used as reinforcement. Compared to conventional engineering materials, these composites offer higher stiffness and strength, especially at elevated temperatures, low coefficient of thermal expansion and enhanced resistance to fatigue, abrasion and wear. Compared to organic matrix materials, they offer high heat resistance and improved electrical and thermal conductivity.

Graphite-reinforced aluminum can be designed to have near zero thermal expansion in the fiber direction. Aluminum oxide-reinforced aluminum matrix composites have been extensively used in automotive connecting rods to provide high stiffness with low weight. Aluminum reinforced with silicon carbide whiskers has been fabricated into aircraft wing panels , providing 20-40% weight saving .Fiber reinforced super alloy has potential future for applications such as turbine blades.

1.3.3 CERAMIC MATRIX COMPOSITE (CMC): Ceramic matrix composites possess properties like high melting points, good corrosion resistance, stability at elevated temperatures and high compressive strength. These materials can even be used at very high temperatures (i.e. above 1500°C).

1.3.4 CARBON –CARBON COMPOSITE: These composites retain their properties even at exceptionally very high temperatures in the range of 3315°C. Their dimensional stability is also good and therefore can be used at elevated temperatures. They are 20 times stronger and 30% lighter than the Graphite fibers. Carbon by itself is brittle and flaw sensitive like the ceramics. Reinforcement of the carbon matrix allows the composite to fail gradually and also gives advantages such as ability to withstand high temperatures, low creep at high temperatures, low density, good tensile and compressive strengths, high fatigue resistance, high thermal conductivity and high coefficient of friction.

1.4 ALUMINUM /ALUMINUM ALLOY BASED MMCS

In research and development as well as in various industrial applications, MMCs based on aluminum and their alloys are widely used [26].This is because aluminum is light in weight which is the primary requirement in most of the applications of the metal matrix composites. Additionally, it is economical in comparison with other light metals, such as titanium and magnesium. Further its excellent strength, ductility and corrosion properties are well established and they can be modified to fulfill the requirements of various applications ranging from automotive and aircraft industry to sports and leisure. The development work of aluminum matrix composite is currently concentrated on two sectors:

(i) Continuous fiber reinforced composite with superior properties for specific applications.

(ii) Mass production technologies of inexpensive discontinuously reinforced composites with moderate properties for wider range of applications. Metal matrix composites possess set of properties that are of interest to the designers for application of both, structural and non-structural nature.

1.4.1 PROPERTIES OF ALUMINUM BASED MMCS: [26]

1.4.1.1 SPECIFIC STIFFNESS**: -** The addition of stiff metallic or ceramic reinforcement materials to the metal matrix results in an increase in elastic modulus of the composites materials. In case of light weight metals, such as aluminum, titanium and magnesium, the increase can be very significant even at moderate levels of reinforcement addition. Typical ceramic reinforcements are similar in density to the light weight metal matrices, and one of the primary benefits of these is their increased specific stiffness.

1.4.1.2SPECIFIC STRENGTH**: -** In addition to high stiffness, aluminum based MMCs also possess high strength. The strength of the composite is strongly dependent on the specific characteristics of the reinforcement material, their morphology, and the type of bonding with the metal matrix. Continuous fiber reinforced composites exhibit high specific strength levels in the direction of the fiber orientation. Particulate reinforced MMCs exhibit specific strength ranging up to double over the metal matrix depending on the matrix alloy as well as reinforcement type and their volume fraction.

1.4.1.3 FATIGUE RESISTANCE**: -** The addition of reinforcement in aluminium/aluminium alloy matrix significantly improves the fatigue resistance. The mechanisms of fatigue resistance enhancement differ in composites depending on the morphology of the reinforcement and characteristics of reinforcement-matrix interface.

1.4.1.4 COEFFICIENT OF THERMAL EXPANSION**: -** The typical ceramic reinforcements for MMCs have significantly lower values of the coefficient of thermal expansion than the metal matrix into which they are incorporated. Thus, the addition of ceramic reinforcement to the high expansion metals such as aluminum, magnesium, copper, and titanium can result in substantial reduction in the coefficient of thermal expansion.

1.4.1.5 WEAR RESISTANCE**: -** The increased hardness of the typical, ceramic reinforcement materials can also affect the tri-biological properties of the metal matrix composites relative to the unreinforced matrix. However the MMCs based on light metals (aluminum, magnesium and titanium), due to lack of wear resistance have limited applications in areas where weight saving could be potentially obtained. Particle reinforced MMCs have been of particular interest for use in wear resistance dominated applications.

1.5 CHARACTERISTICS OF COMPOSITE MATERIALS

As explained earlier, there are three items that determine the characteristics of a composite: the reinforcement, the matrix, and the interface between them. The constituents of a composite are arranged so that one or more discontinuous phases are embedded in a continuous phase. The discontinuous phase is termed the ***reinforcement*** and the continuous phase is the ***matrix.*** In general the reinforcements are much stronger and stiffer than the matrix. But both constituents are required and each must accomplish specific tasks. A material is generally stronger and stiffer in fiber form than in bulk form. The strength of the fiber is greater than that of the bulk material.

Without a binder material to separate them, they can become knotted, twisted, and hard to separate. The matrix material must be continuous and surround each fiber so that they are kept distinctly separate from adjacent fibers and the entire material system is easier to handle and work with. The physical and mechanical properties of composites are dependent on the properties, geometry, and concentration of the constituents. Increasing the volume content of reinforcements can increase the strength and stiffness of a composite to a point. If the volume content of reinforcements is too high there will not be enough matrix to keep them separate, and they can become tangled.

1.6 FACTORS TO BE CONSIDERED WHEN DESIGNING COMPOSITE MATERIALS

- The type of reinforcement and matrix,
- The geometric arrangement
- Volume fraction of each constituent,
- The anticipated mechanical loads,
- The operating environment for the composite, etc.

Isotropic, homogeneous materials (steel, aluminum, etc.) are assumed to be uniform throughout and to have the same elastic properties in all directions. Upon application of a uniaxial tensile load, an isotropic material deforms in a manner similar to that indicated in Figure 1.5(the dashed lines represent the un-deformed specimen). Assuming a unit width and thickness for the specimen, the transverse in-plane and out-of-plane displacements are the same. Unlike conventional engineering materials, a composite material is generally non-homogeneous and does not behave as an isotropic material. **Most composites behave as either *anisotropic* or *orthotropic* materials.**

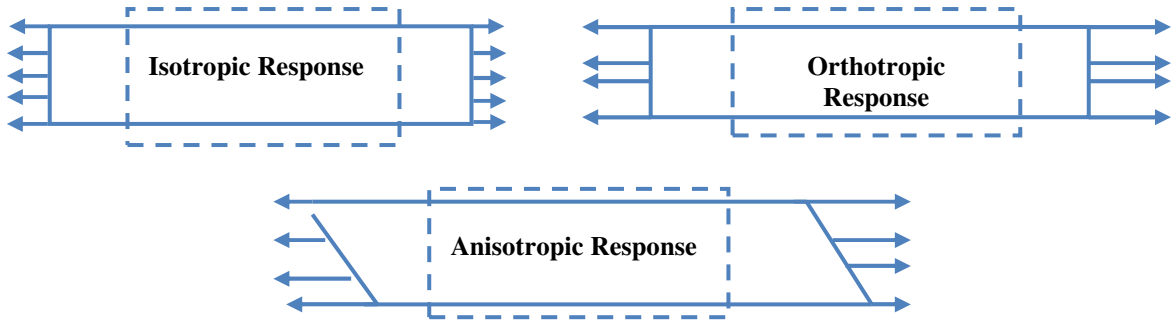

Figure 1.6 Isotropic, anisotropic and orthotropic responses subjected to axial tension.[33]

The material properties of an anisotropic material are different in all directions. There is typically a coupling of extension and shear deformation under conditions of uni-axial tension. The response of an anisotropic material subjected to uni-axial tension is also illustrated in Figure 1.6**.** There are varying degrees of anisotropic material behavior, and the actual deformation resulting from applied loads depends on the material. The material properties of an orthotropic material are different in three mutually perpendicular planes. The transverse in-plane and out-of-plane displacements are not typically the same, because Poisson's ratio is different in these two directions. Figure 1.6also illustrates orthotropic material response. Although it appears similar to that of an isotropic material, the magnitudes of the in-plane and out-of-plane displacements are different.

1.6 FUNDAMENTAL COMPOSITE MATERIAL TERMINOLOGY

1.7.1 LAMINA: - Alamina is a flat (or sometimes curved) arrangement of unidirectional (or woven) fibers suspended in a matrix material. A lamina is generally assumed to be orthotropic, and its thickness depends on the material from which it is made. For the purpose of analysis, a lamina is typically modeled as having one layer of fibers through the thickness. Both unidirectional and woven lamina is schematically shown in Figure 1.7.

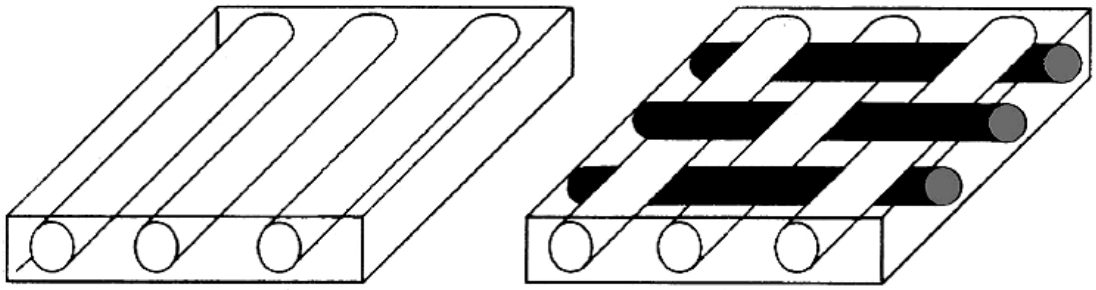

Uni-directional Woven

Figure 1.7 Schematic representation of unidirectional and woven composite lamina. [33]

1.7.2 REINFORCEMENTS: - Reinforcements are used to make the composite structure or component stronger. The most commonly used reinforcements are boron, glass, graphite (often referred to as simply carbon), and Kevlar. There are some other types of reinforcements such as alumina, aluminum, silicon carbide, silicon nitride, and titanium.

1.7.3 FIBERS: - Fibers are a special case of reinforcements. They are generally continuous and have diameters ranging from 120 to 7400 pin (3-200 μm). Fibers are typically linear elastic or elastic-perfectly plastic and are generally stronger and stiffer than the same material in bulk form. The most commonly used fibers are boron, glass, carbon, and Kevlar.

1.7.4 MATRIX: - The matrix is the binder material that supports, separates, and protects the fibers. It provides a path by which load is both transferred to the fibers and redistributed among the fibers in the event of fiber breakage. The matrix typically has a lower density, stiffness, and strength than the fibers. Matrices can be brittle, ductile, elastic, or plastic. They can have either linear or nonlinear stress-strain behavior. The most commonly used matrices are carbon, ceramic, glass, metal, and polymeric. Each has special appeal and usefulness, as well as limitations.

1.7.4.1 CARBON MATRIX**:**

a) Have a high heat capacity per unit weight.
b) Used as rocket nozzles, ablative shields for reentry vehicles, and clutch and brake pads for aircraft.

1.7.4.2 CERAMIC MATRIX**:**

a) Usually brittle.

b)Carbon, ceramic, metal, and glass fibers are typically used with ceramic matrices in areas where extreme environments (high temperatures, etc.) are anticipated.

1.7.4.3 GLASS MATRIX**:**

a) Usually have an elastic modulus much lower than that of the reinforcement.

b) Carbon and metal oxide fibers are the most common reinforcements with glass matrix composites.

c) The best characteristics of glass or ceramic matrix composites are their strength at high service temperatures.

d) The primary applications of glass matrix composites are for heat-resistant parts in engines, exhaust systems, and electrical components

1.7.4.4 METAL MATRIX**:**

a) Especially good for high-temperature use in oxidizing environments.

b) Most commonly used metals are iron, nickel, tungsten, titanium, magnesium, and aluminum.

1.7.4.5 POLYMER MATRIX:

a) Most common and least expensive

b)Polymers are easy to process

c) Offer good mechanical properties

d) Generally wet reinforcements well, and provide good adhesion.

e)They are a low-density material because of low processing temperatures many organic reinforcements can be used

A typical polymeric matrix is either visco-elastic or visco-plastic, meaning it is affected by time, temperature, and moisture. The terms thermo-set and themo-plastic are often used to identify a special property of many polymeric matrices.

1.7.4.5.1 THERMO-PLASTIC: - A thermoplastic matrix has polymer chains that are not cross-linked. Although the chains can be in contact, they are not linked to each other. A thermoplastic can be remolded to a new shape when it is heated to approximately the same temperature at which it was formed.

1.7.4.5.2 THERMO-SET: - A thermo-set matrix has highly cross-linked polymer chains. A thermo-set cannot be remolded after it has been processed. Thermo-set matrices are sometimes used at higher temperatures for composite applications.

1.8SOME APPLICATIONS OF COMPOSITES[27]

This is a brief listing of current and proposed applications of composite materials in various branches of industry. It is not intended to be comprehensive or all-embracing, but merely to give an indication of the range of possibilities for designers

1.8.1 AEROSPACE: They are used in air frames, wing spars, spoilers, tail-plane structures, fuel tanks, drop tanks, bulkheads, flooring, helicopter rotor blades, propellers, and structural components, pressured gas containers, radomes, nose and landing gear doors, fairings, engine nacelles (particularly where containment capability is required for jet engines), air distribution ducts, seat components, access panels, and so forth. Many modern light aircraft are being increasingly designed to contain as much lightweight composite material as possible.

1.8.2 AUTOMOTIVE ENGINEERING: Reduction in the weight of an automobile structure achieves primary weight-saving and if carried to sufficiently great lengths enables the designer to use smaller power plants, thus achieving substantial secondary improvements in fuel economy. A

wide range of car and truck body mouldings, panels and doors is currently in service, including complete front-end mouldings, bumper mouldings, and various kinds of trim. There is considerable interest in the use of controlled crush components based on the high energy-absorbing qualities of materials like GRP. Leaf and coil springs and truck drive shafts are also in service, and GRP wheel rims and inlet manifolds have been described in the literature. Selective reinforcement of aluminium alloy components, such as pistons and connecting rods, with alumina fibres is much discussed with reference to increased temperature capability.

1.8.3 BIO ENGINEERING: Pyrolytic carbon is used to manufacture heart valve components, and the substitution of a carbon/carbon composite is not unlikely. There have also been developments in the use of particulate hydroxyapatite as filler in a thermoplastic composite for bone re-modelling or replacement

1.8.4 CHEMICAL ENGINEERING: A substantial amount of GRP is currently in use in chemical plant for containers, pressure vessels, pipe-work, valves, centrifuges etc. These may be filament-wound or moulded components for containment of process fluids.

1.8.5 CIVIL/STRUCTURAL ENGINEERING: In recent years there has been a major surge of interest in the use of structural composites in civil engineering infrastructures. The low inherent elastic modulus of GRP is easily overcome in buildings by the use of double curvature and folded-plate structures: thin GRP panels also offer the advantage of translucency. A good deal of GRP is used in this industry for folded-plate structures, cladding panels, decorative 'sculptured' panels (like those in the doors of the Roman Catholic cathedral in Liverpool), services mouldings and ducting, racking, pipework, rainwater mouldings, domestic and industrial water tanks, form-work for concrete, and complete small structures like foot-bridges. Light-weight composite panelling for partitioning and similar applications have also been tried. CFRP have been less used until recently because of the cost, but are increasingly being considered for building light-weight structures, including a number of bridges.

1.8.6 DOMESTIC: Injection-moulded reinforced thermoplastics and polyester moulding compounds are perhaps the most common composites used in consumer items for the domestic market, and the range is vast. Mouldings of all kinds, from kitchen equipment of all kinds to casings for the whole gamut of domestic and professional electrical equipment, motor-cycle crash helmets, television and computer casings, and furniture.

1.8.7 ELECTRICAL ENGINEERING: Typical applications are radomes, structural components for switch gear, power generator coolant containment and large-diameter butterfly valves, high-strength insulators (*e.g.* for overhead conductor systems), printed circuit boards, and casings for electronic equipment. The majority of applications in this field again use GRP, although the use of composites which are more thermally stable and more moisture-resistant is increasingly predicated for sensitive, small-scale electronic components.

1.8.8 MARINE ENGINEERING: Marine applications include surface vessels, offshore structures and underwater applications. A vast range of pleasure craft has long been produced in GRP, but much serious use is also made of the same materials for hull and superstructure construction of passenger transport vessels, fishing boats and military (mine-countermeasures) vessels. Sea-water cooling circuits may also be made of GRP as well as hulls and other structures. Off-shore structures such as oil rigs also make use of reinforced plastics, especially if they can be shown to improve on the safety of steel structures, for fire protection piping circuits, walkways, flooring, ladders, tanks and storage vessels, blast panels, and accommodation modules.

1.8.9 SPORT: the most visible development in the use of composites has been in the sports goods industry.GRP vaulting poles were perhaps the earliest of the composite sports gear, but one can now obtain tennis rackets, cricket bats, golf clubs, fishing rods, boats, oars, archery equipment, canoes and canoeing gear, surf boards, wind-surfers, skateboards, skis, ski-poles, bicycles, and protective equipment of many sorts in composite materials of one kind or another.

1.9FUNCTIONALLY GRADED MATERIALS AND THEIR USES

Beyond a vast usage of these composite materials, yet there is one special class of materials designed for the purpose of taking desired requirement by retaining their variable distribution in the fog the other reinforced material. This special class of materials is known as functionally graded materials. The Latest developments in engineering materials have permitted the use of these inhomogeneous materials FGMs in structural elements. Functionally graded materials are also heterogeneous composite materials with gradient compositional disparity of the constituents (e.g. metallic and ceramic) from one surface of the material to the other which results in constantly varying material properties. As earlier explained, the materials are purposefully designed in such a way that they possess desired properties forchosen specific applications. The

concept of FGM, initially developed for super heat resistant materials to be used in space planes or nuclear fusion reactors, is now of interest to designers of functional materials for energy conversion, dental and orthopedic implants, sensors and thermo generators [12]. Additional potential applications of FGMs include their use as interfacial zones to improve the bonding strength and to reduce residual stresses in bonded dissimilar materials and as wear resistant layers such as gears, cams, ball and roller bearings and machine tools. The variation of material properties in an FGM is usually obtained by changing the volume fractions of two or more compatible constituents. A.M.Zenkour [2] have presented stress distribution in a rotating disk problem for functionally graded materials with the help of two disk structures. A study of thermal stresses in a rotating FG hollow circular disk was carried out by Xu-Long Peng*et al*.[23]. H.Callioglu*et al*.[8]examined stress analysis of annular rotating discs made of functionally graded materials (FGMs) and gave analytical and numerical solutions. Whereas H. Callioglu alone[7] presented an analytical thermo-elasticity solution for a disc made of functionally graded materials (FGMs) by using Infinitesimal deformation theory of elasticity and power law distribution for functional gradation. M.Damircheli*et al*. [11]carried out radial and hoop thermal and mechanical stress analysis of a rotating disk made of functionally graded material (FGM) with variable thickness by using finite element method (FEM). Xu-Long Peng*et al*.[24] gave elastic analysis of a rotating sandwich solid disk composed of three-layered perfectly-bonded composites by considering two cases in which one is on FGM with power-law gradient and the other is on FGM with any radial non-homogeneity. M. Bayat*et al*. [10] presented the theoretical formulation for bending analysis of functionally graded (FG) rotating disks based on first order shear deformation theory (FSDT).

1.10 CREEP: Any specimen of certain material when subjected to a constant load, it deforms continuously (Fig. 1.8). The material will carry on deforming slowly with time or until rupture or yielding causes failure. This phenomenon of deformation under load with time is known as creep. In other words *"Creep is the tendency of a solid material to move slowly or deform permanently under the influence of long time stresses"*. Creep is more severe in materials that are subjected to heat for long periods, and near melting point. Creep always increases with temperature. Unlike brittle fracture, creep deformation does not occur suddenly upon the application of stress. Instead, strain accumulates as a result of long-term stress. So, creep is a

"time-dependent" deformation. The rate of this deformation is a function of the material properties, exposure time, exposure temperature and the applied structural load. There are three stages of creep as follows:

1. STAGE 1: PRIMARY REGION: In the early stage, or primary creep, the strain rate is relatively high, but slows with increasing time. The primary region is the early stage of loading when the creep rate decreases rapidly with time. This is due to work hardening
2. STAGE 2: SECONDARY REGION: The strain rate eventually reaches a minimum and becomes near constant. This is due to the balance between work hardening and annealing (thermal softening). This stage is known as secondary or steady-state creep. This stage is the most understood. The characterized "creep strain rate" typically refers to the rate in this secondary stage. Stress dependence of this rate depends on the creep mechanism.
3. STAGE 3: TERTIARY REGION: In tertiary creep, the strain rate exponentially increases with stress because of necking phenomena i.e. rapid increase and fracture.

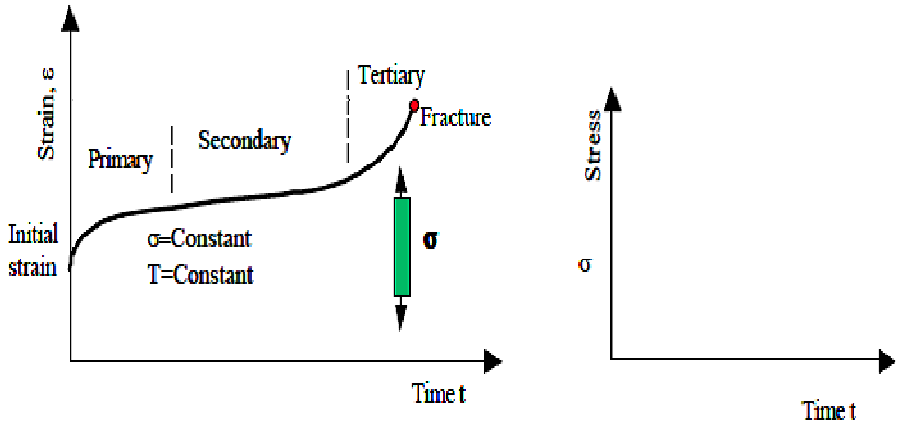

Figure1.8 Creep Stages[34]

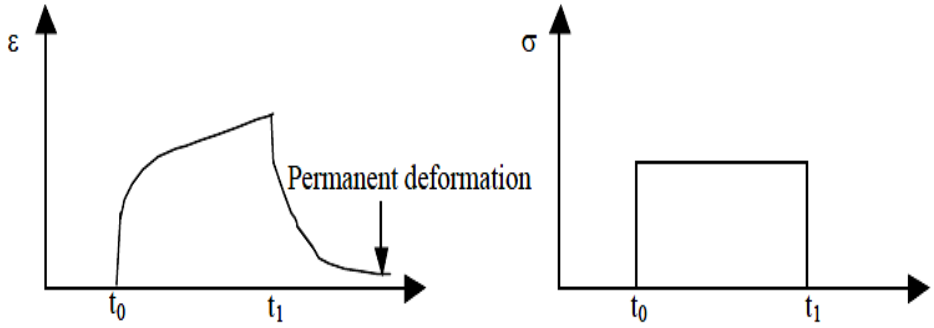

Figure 1.9 Creep curve, a constant load is applied[34]

If the functional load is released before the creep rupture occurs, an immediate elastic retrieval equal to the elastic deformation, followed by a period of slow recovery is observed (Figure 1.9). The material in most of the cases does not recover to the original shape and a permanent deformation always remains. To measure creep a test named creep rupture test is usually kept on experimented. The creep rupture is basically similar to a creep test with the exception that it is continued until the material flops. This test is useful in establishing a safe envelope inside a creep test. The basic information obtained from the stress rupture test is that the time to failure at a given stress. Based on this data, a safe stress can be determined under which it is safe to operate, given the time requirement of the end use application. The construction of the creep rupture envelope is shown in Figure 1.10. Test is conducted under constant stresses and the points of the commencement of tertiary stage are connected to form the creep rupture envelope.

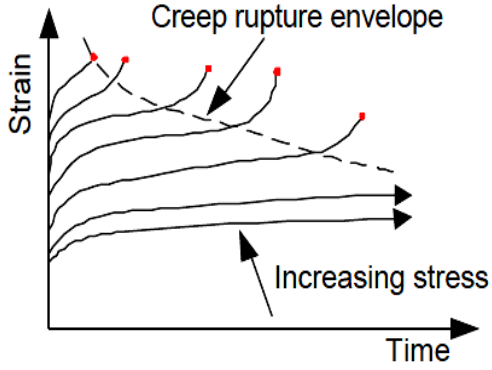

Figure 1.10 Creep rupture envelope [34]

1.11 CREEP LAW

Let us consider a rotating disc of functionally graded material composed of aluminium matrix reinforcement with silicon carbide i.e. Al–SiC_p, is supposed to undergo steady state creep following the well-documented creep law, which is given by,

$$\dot{\bar{\varepsilon}} = \frac{A}{\bar{\sigma}} \left(\bar{\sigma} - \sigma_{th} \right)^{n} \exp\left(-\frac{Q}{RT} \right)$$

where the symbols $\dot{\bar{\varepsilon}}$, $\bar{\sigma}$, σ_{th}, A, n, Q, E, R, and T denote respectively the effective strain rate, effective stress, threshold stress, structure-dependent parameter, true stress exponent, true activation energy, temperature- dependent Young's modulus, gas constant, and operating temperature.

Alternatively, the creep law [19] may also be written as

$$\dot{\bar{\varepsilon}} = [M(\overline{\sigma} - \sigma_0)]^n \ldots\ldots\ldots\ldots\ldots\ldots\ldots\ldots\ldots\ldots (1.2)$$

$$\text{where } M = \frac{1}{E}(A' exp\frac{-Q}{RT})^{1/n} \ldots\ldots\ldots\ldots\ldots\ldots\ldots\ldots\ldots\ldots (1.3)$$

M and σ_0 acting in equation are the creep parameters describing steady state creep behavior, and are dependent on the dispersoid content size, exposed temperature and particle content volume employed whereas the parameter n in the above equation is termed as true stress exponent or simply stress exponent. The value stress exponent n is usually kept as 3, 5 or 8 which correspond to the following [28][30][31][32] three well-known creep cases [5]:

a) n=3 for creep controlled by viscous glide processes of dislocation
b) n =5 for creep controlled by high-temperature dislocation climb (lattice diffusion)
c) n =8 for lattice diffusion-controlled creep with a constant structure.

CHAPTER 2

LITERATURE REVIEW

The applications of composite materials and functionally graded materials are increasing scope in engineering, mostly in structural applications and several relatively new features of materials behavior are being addressed. For example, the long term behavior under mechanical, thermal and chemical/environmental loadings. The contemporary study concerns the creep performance, which is of significant interest. The investigational testing and valuation of the many available composite material systems are very complex, costly as well as time consuming. Therefore, the prediction and analysis of creep stuffs for the assessment of service life of the components made of composite materials, is of great practical significance for working engineers.

2.1 ROTATING DISK: Rotating discs have been getting considerable attention owing to their wide range of engineering applications in rotating machinery. Applications of these rotating discs lie mainly in the following areas:

1. Gas turbine (stationary and on aircraft) whose blades operate at a temperature of 800-950 K. the burner and after burner sections operate at even higher temperature viz. 1300-1400 K.
2. Nuclear reactor where pressure vessel and piping operate at 650-750 K. Reactor skirts operates at 850-950K.
3. Chemical and petrochemical industries.
4. Pumps, compressors, flywheels, automotive, railway, aerospace braking systems etc.

All of these, temperatures are in the range of (0.4-0.65) T_m, where T_m is the melting point of the material in kelvin. In most of these applications, the disc is subjected to severe mechanical and thermal loadings, thereby leading to creep deformations of the disc material. The excellent mechanical properties, such as high specific strength and stiffness and high temperature stability, offered by aluminium-based composites consisting of silicon carbide (SiC) particles, whiskers, or fibres make them an appropriate material for use in rotating disc applications exposed to elevated temperature. The experimental and theoretical studies accompanied so far also reveal that the steady state creep rate in metal matrix composites discs based on aluminium or its alloys reinforced with ceramic particles, is reduced by several orders of magnitude when compared

with pure aluminium or its alloys. A rotating disc at elevated temperature is a common component in aero-engines, automobiles, turbines, pumps, compressors and in a number of other dynamic applications. A reduced weight of such components, resulting from the use of aluminium/aluminium base alloys, is expected to save power and fuel due to a reduction in the payload. However, the enhanced creep of aluminium and its alloys may be a big hindrance in such applications. Particle and whisker-reinforced metal matrix composites have shown superior high temperature properties and are finding increasing application in components exposed to higher temperature. Earlier study conceals that aluminium matrix based composite has better creep resistance compared to the base aluminium alloy. The study pertaining to steady state creep behavior of Al–SiC_p composites under uniaxial condition in the temperature range between 623–723 K for different particle sizes and with varying volume fraction of reinforcement indicated that the composite with finer particle size has better creep resistance than that containing coarser ones. [28]

2.2 YIELD CRITERIA FOR DUCTILE MATERIALS

Aluminum based reinforced materials are ductile in nature, therefore this section discusses the yield criteria applicable for ductile materials. Thus when a material is simultaneously acted upon by a complex system of stresses i.e. when it is subjected to three principal stresses; it becomes important to know how the elastic failure will occur. It may further be pointed out that these theories relate to such stresses, often called the static stress and not necessarily to either suddenly applied loads or stresses which fluctuate cyclically and are applied repeated[29]. Whatever the system of stress applied to a body, it can always be resolved into three principal stresses, σ_1, σ_2 and σ_3 (say). In the discussion it will also be assumed that, $\sigma_1 > \sigma_2 > \sigma_3$.

2.2.1MAXIMUM SHEAR STRESS THEORY: The assumption in this theory is that yielding is dependent on the maximum shear stress in the material reaching a critical value. This latter value is taken as the maximum shear stress in a simple tensile test, which is half the yield stress, or $\frac{1}{2}\sigma_t$. The maximum shear stress in the complex stress system will depend on the relative values and sign of the three principle stresses, always being half the difference between the maximum and minimum. For general three-dimensional stress system, or in the two-dimensional case with one of the stresses compressive and the other tensile, the maximum shear stress is

$$\hat{\tau} = \frac{\sigma_1 - \sigma_3}{2} \text{ and for yielding } \frac{\sigma_1 - \sigma_3}{2} = \frac{\sigma_t}{2} \text{ or } \sigma_1 - \sigma_3 = \sigma_t$$

In a two dimensional stress system when σ_3=0, i.e. for σ_1 and σ_2 tensile, the maximum difference between the principal stress is

$$\hat{\tau} = \frac{\sigma_1 - 0}{2} = \frac{\sigma_1}{2} \text{ and yielding occurs if } \frac{\sigma_1}{2} = \frac{\sigma_t}{2} \text{ or } \sigma_1 = \sigma_t$$

This theory is usually coupled with the names of **Guest and Tresca Theory**

2.3 LITERATURE SUMMARY

In context to the above investigation a wide range of literature has been conducted in line with the titled research plan to find out the updated research performed till date and finding out the gaps in the literature. The following is the exploration works referred:

Wahl *et al.* [1] carried out an experimental and theoretical study on steady state creep behavior of rotating disc at higher temperature made up of steel. A mathematical formulation was also established for theoretic calculation of creep effects for the comparison with experimental results. Theoretical results were calculated by using Von-Mises and maximum shear stress theory. It was suggested out that the available methods of calculating creep results were somewhat lower when Von-Mises criterion was followed than using shear stress theory. The later would give slightly higher values of stress but within the safe limits.

Shukla[13] identified the creep stresses in thin rotating annular disc made up of non-homogeneous material by transition theory. It was observed that the presence of non-homogeneity having lesser value at the bore, reduced the stresses and angular velocity required for steady state creep as compared to the homogeneous disc. Higher value of presence of non-homogeneity at the bore than at the rim, increased the magnitude of angular velocity and creep stresses significantly, and increased the possibility of a facture in the vicinity of the bore.

Singh *at el.*[15] observed the steady state creep strain rate response of an isotropic FGM rotating disc made of 6061 Al alloy strengthened with linearly varying volume fraction of SiC, improved from the outer to inner radius. To describe the steady state creep, Norton's laws was used to obtain the steady-state creep response of the composite discs (i) with uniform particle content (Non-FGM disc) and (ii) with particle gradient (FGM disc) rotating at 15000 rpm at 561K. It was observed that in FGM disc, tangential stresses near the inner radius were more with higher

particle gradient but near the outer radius stress distribution were lessened as compare to FGM disc. Radial stresses were observed higher in the middle of the FGM disc as compare to non FGM disc, when disc has higher particle gradient distribution. Creep parameters were reduced due to increased particle gradient near the inner radius but near the outer radius tangential creep rates were also lessened due to lower particle content. Radial strain rate (compressive) reduced in FGM disc as the gradient distribution increased. It was observed that in a rotating disc radial and tangential stresses can be controlled by increasing the particle contents thereby reducing the creep results also.

Gupta *et al.* [19] studied steady state creep in a rotating disc made of isotropic composites containing SiC particles in an aluminium matrix. Sherby's constitutive model which was claimed better than Norton's creep model was used to describe the creep behavior of the composite. It was also observed that the material parameter affects the stresses both radial and tangential. The tangential stresses increased rapidly and reached maximum value before decreasing near the outer radius. The radial stress found maximum somewhere near the middle of the disc. Particle size & particle content played an important role. It was detected that creep rate at any radius reduced by almost three order of magnitude when particle size decreased from 45.9µm to 1.7µm. when the particle content changes from 10 vol. % to 30 vol. % the maximum variations was observed in tangential stresses. It was about 5%. Radial stresses not affected significantly over entire radius. In this maximum variations were observed to be 1%. Significant change was observed in tangential and radial strain rates, for given particle content. Temperature also affected the system of stresses i.e. 623K, 673K, and 723K. A very little effect was found in radial stress distribution when temperature was varied. The max difference was found in tangential and radial stresses which were only about 0.15%. The variation was observed in tangential strain rates and radial strain rates. Tangential strain rate increased by three orders of magnitude when temperature varied from 623K to 723K.

Singh *et al.* [16] described the steady state creep response in an isotropic FGM rotating disc of Al SiC particulate composites with composition gradient along the radial direction by using Norton's law. To obtain the steady-state creep response of the composite discs (i) with uniform particle content (Non-FGM disc) and (ii) with particle gradient (FGM disc) rotating at 15000 rpm at 561K were used. Tangential stresses found maximum at the inner radius and minimum at the

outer radius in FGM disc as compare to Non-FGM disc, when particle contents decreasing from inner to outer radius. Radial stresses found maximum at somewhere middle of the disc. Drastically change in tangential strain rates was observed in Non-FGM disc as compare to FGM disc. Radial strain rates found tensile at the middle of the disc in FGM disc, but found compressive inner to outer radius in Non-FGM disc (Fig. 12).

Gupta*et al*. [20] examined creep behavior of a rotating disc made of isotropic FGM disc made of composite containing silicon carbide particles in a matrix of pure aluminum. The creep behavior had been defined by Sherby's law. The disc was considered as having a thermal gradient in the radial direction. In an isotropic rotating FGM Disc with linearly decreasing particle content from the inner to the outer radius, the steady-state creep response in terms of strain rates is superior to that in a disc with uniform particle content when both the discs have the same average particle content and are under similar thermal gradient. The steady-state creep responses of both FGM and uniform composite discs under thermal gradient are superior to those under isothermal condition, but the response of the FGM disc is better than that of uniform disc under the imposed thermal gradient having the same average as the isothermal temperature and in the uniform composite disc, a combination of higher tangential stress and lower temperature near the inner radius of the disc and higher temperature and lower tangential stress near the outer radius results in overall decrease in creep rates over the entire disc. Higher particle content near the inner radius and lower particle content near the outer radius of the FGM disc further reduces the creep rate, making its creep response even better.

Singh *at el*.[17] investigated steady state creep for anisotropic rotating composite disc having residual stresses, following the criterion of yielding. It was observed that tangential stresses developed due to rotation lowered value in the middle of the disc as compared to the disc without residual stresses. But stresses were higher in the region near the inner and outer radii. Radial stresses developed due to rotation, in the disc with residual stresses was similar to that in the disc without residual stresses. Tangential creep rates increased significantly as compared to the disc without residual stresses. The increased creep rate was more near the inner radius as compared to outer radius. It was observed that magnitude of residual stresses which as tensile made radial strain rate tensile at the middle of the disc while it remained compressive near the inner and outer radius. Residual stresses caused significant distortion in the disc.

Gupta *et al.* [21] examined interrelation of thermal as well as composition gradient in the context of creep behavior of rotating disc developing stresses due to its rotation. A rotating isotropic FGM aluminium disc having an average silicon carbide content of 20 vol. % distributed linearly in the radial direction, decreased from inner radius to outer radius, was subjected to a thermal gradient in order to study its creep response following Sherby's creep law. Obtained results were compared with those obtained following Norton's creep law. In this study the temperature profile determined for a given particle distribution by FEM technique. It was observed in disc 1 with both particle gradient and thermal gradient resulting from braking action of FGM disc (V_{max}=30 vol. % and V_{min}. =13.6 vol. %), higher particle gradient resulted in relatively higher thermal gradient although the end temperatures did not changed significantly. It was also observed that tangential stresses and radial stresses were maximum which was obtained by Sherby's law as compared to Norton's results. The maximum difference was found 10%. Radial strain rates did not differ significantly but near the inner radius difference was found. The maximum difference was between both laws was 22%.

Singh[22] investigated the stress distribution and the creep strain rates, in the isotropic 6061Al base alloy and the composite of the same base alloy containing 20 vol. % of SiC_w whiskers. It was observed that variation in radial stresses in case of isotropic disc 6061Al base alloy and the composite of the same base alloy containing 20 vol. % of SiC. Disc was rotating at 15000 rpm at 516K. It was observed that variation in radial stresses in case of isotropic disc, was zero. At inner and outer radius, but observed higher radial stresses in Al alloy as compared to composites. Lower radial distance (inner radius) tangential stresses were higher in Al alloy as compared to composites but at outer periphery tangential stresses were higher in composites as compared to Al alloy. Radial strain rate (compressive) in composites was about three orders of magnitude lower than the strain rate in the Al alloy. Radial strain rate in the middle of the disc was less in comparison to those at inner and outer radius or periphery. Variation in tangential strain rate at a given condition was observed. Variations in radial and tangential stresses and radial and tangential strain rates in anisotropic disc were also observed. Assumptions which were taken to obtain the results were F/H = 1, where F and H were Hill's anisotropic constants. It was found that if parameter (α) is less than one implies that strengthening in tangential direction, if greater than one implies weakening in tangential direction, if less than unity radial stresses increased near the inner periphery and decreases near outer periphery with respect to isotropic case.

Variations were observed when the value of (α) was 0.7, 1.0, 1.3. Radial strain rate remains compressive for isotropic case when the value of α was 1. It became tensile in the middle region of the disc when α greater than 1 and less than 1.

Zenkour[2]examined stress distribution in rotating composite structures of functionally graded solid disc. Accurate analytical solution obtained for the rotating of disc structures subjected to different conditions. Two composite structures of functionally graded material (FGM) solid disks were considered. The composite structures were composed of three-layer sandwich solid disks with faces made of different isotropic materials and core made of FGM. For Structure 1, the inner layer was metal and the outer layer was ceramic while the core layer is a metal–ceramic FGM. Structure 2 was composed of the same constituent materials as in Structure 1 but interchanging the inner layer of metal material with the ceramic one. The stresses and displacement distributions were smooth through the radial direction of the composite disks. The circumferential stresses for some structures of the clamped and free FG disks were found to be maximum.

Baya*t al*. [10] presented the theoretical formulation for bending analysis of FG rotating disks founded on first order shear deformation theory. The material properties of the disk were supposed to be graded in the radial direction by a power law. A set of new equilibrium equations were developed with small deflections. Three types of boundary conditions were applied. Acquired results were compared with recognized results reported in the literature. Mechanical comebacks were also compared between homogeneous and FG disks. It was found that the stress couple resultants in a FG solid disk were not as much of the stress resultants in full-ceramic and full-metal disk. The vertical displacement in a FG mounted disk with free condition at the outer surface was found to be greater than the vertical displacement in a full-metal disk. It might be concluded from this effort that the gradation of the constitutive components is an important parameter that may affect the mechanical responses of FG disks. For different combinations of FG disks dimensionless deflection, stress and moment resultants were calculated. Elastic stresses and displacement for the solid disk with a roller support at outer radius and the hollow disk with fastened inner edge and roller at the external edge or free boundary conditions were found. Results were presented for solid and hollow disks with thickness and outer radius ratio taken and for different values of the grading index n of material properties. For the FG disk using

aluminum as the inner surface metal and zirconia as the outer surface ceramic material the numerical results were obtained for both.

Tutuncu *et al.* [13] determined axisymmetric displacements and stresses via plane elasticity theory and Complementary Functions method in functionally-graded hollow cylinders, disks and spheres subjected to uniform internal pressure. The material expected to be functionally graded in the radial direction. Dissimilarities in the material properties such as Young's modulus and Poisson's ratio may be arbitrary functions of the radial coordinate. This assumption yielded a two-point boundary value problem with a governing differential equation of flexible coefficients. CFM reduced the boundary value problem to an initial-value problem which could be resolved accurately by one of many capable methods. A number of material models from the literature were used and conforming radial displacement and stresses were calculated. Authentication of the proposed method was done using benchmark solutions available in the literature for some special cases. The governing equations of cylinder, disc and spheres were obtained and then these equations converted into initial value problems and then solved by CFM. Using CFM, radial displacements, radial stress and hoop stress were calculated and then were compared with the analytical results. It has been appreciated that the results that were compared with the analytical results, were very much parallel infact exactly same as that of analytical results. The non-dimensional radial displacement, radial stress and hoop stress were all calculated for a unit inner pressure and plotted in the form of graphs by assuming the FGM model with constant Poisson's ratio and Young's modulus varying as a single power law.

Rattan *et al.* [12] investigated creep response for isotropic axisymmetric rotating disc made of a particle-reinforced FGM. The disc under study was made of Al-SiC particulate composite. The result developed for nonlinear difference of particle dispersal along the radial distance of the disc were compared with that of discs comprising the same amount of particle distributed uniformly or linearly along the radial distance. To describe the Creep behavior of the disc Sherby's law was used. The material parameters of creep varied along the radial distance in the disc due to varying composition, and this variation had been assessed by regression fit of the available experimental data. It was concluded that a functionally graded rotating disc with parabolic profile can be more effective than those with uniform distribution or linear variations of particle content along the radius.

In this work, the authors evaluated the variations in radial stresses σ_r and tangential stresses σ_θ versus radial distance. To obtain the results, non FGM, FGM linear, FGM non-linear discs were used. It was observed that radial stresses increase as one move from inner radius to the central radial distance and reached maximum nearly at the centre and then decrease towards outer radius of the disc. It was also observed that in all the three types of discs tangential stresses increase from inner radius to outer radius. Tangential stress changed drastically for both FGM discs as move from inner radius to outer radius but small variation was seen in the uniformly distributed particle content.

Deepak *et al.*[4] examined creep behavior in Al-SiC FGM rotating discs made up of changing thickness. The creep behavior of the composite had been described by threshold stress based creep law. The study specified that in the presence of particle gradient in a rotating disc, the tangential stress increases near the inner radius but decreases at the outer radius. In the FGM discs with linearly reducing particle content from the inner towards the outer radius, the steady state creep response in terms of strain rates was superior to that observed in a disc containing uniform distribution of reinforcement, when both the discs have the same average amount of reinforcement. It was also concluded that employing higher particle gradient in the FGM disc, the dispersal of strain rates in the disc became comparatively more uniform.

Peng*et al.*[23] presented a method to resolve the thermo elastic problem of a rotating functionally graded hollow circular disc. The hollow disc was assumed to have varying material properties along the radial direction. An analytical technique was presented to investigate thermal stresses in a functionally graded circular annulus rotating disk with constant angular velocity. He converted the problem in problem to solve a Fredholm integral equation. After solving the Fredholm integral equation, the distribution of the thermal stresses and radial displacement of a rotating hollow disk were obtained. A comparison of the mathematical results with the exact ones confirms the effectiveness of the method for material properties of special power-law profile. Numerical results had been plotted to show in what manner the gradient parameter, temperature change, angular velocity and thickness of disc affect the distribution of the components of stresses and displacement. The method presented in this study was completely different from

previous methodologies available and it helps engineering designers to choose appropriate gradients and materials to acquire an optimum state of a rotating functionally graded hollow disk.

Altan*et al.*[6]carried out the elastic stress analysis with aluminium matrix of a composite disc subjected to a linearly increasing temperature distribution. Two different methods were employed, one is numerically and other is analytically. A computer program has been developed in the analytical analysis to get the values of thermal stresses and in the numerical study the finite-element method is used. As a result of these analyses, it has been observed that the results gained from these two solution methods were very close to each other. Therefore, both of these solution methods had found to support each other. Having different thermal expansions in the orthotropic composite disc, tangential stresses were always on the condition of compression from the inner portions of the disc whereas tensile on the outer side of the disc. Radial stress components were zero in the inner and outer surfaces of the composite disc and remain as tensile in the middle parts of it. It had also been found out that radial stress components were always in the state of tensilealong the entire profile of the disc. Radial and tangential thermal stresses increased by increasing linearly-increasing thermal loads. It has been concluded that the stress values were nearly identical until the (d/r) ratio of 0.2 and the tangential stress components decrease in the inner surfaces and increase in the outer surfaces with the increase in (d/r) ratio.

Afsar*et al.* [3] developed finite element model to analyze the thermo elastic field in a rotating FGM circular disk bearing in mind the incompatible eigen strain developed in the disk due to non-uniform coefficient of thermal expansion and non- uniform temperature distribution. It was found that the thermo elastic field in an FGM disk considerably influenced by the temperature distribution profile, radial thickness, angular speed, and inner and outer surface temperature difference. Thus, the thermo elastic field in an FGM disk can be controlled and optimized by regulating these parameters.

Callioglu*et al.*[8] derived tangential and radial stress equations from the governing differential equation of equilibrium for a thin rotating disc of an aluminum alloy material with FGM is chosen including elasticity modulus E and mass density ρ assumed as a function of r which represents FGMs. Elasticity modulus and density of the discs are assumed to vary radially

according to a power law function, but the material is of constant Poisson's ratio. A gradient parameter n is taken whose value lies between 0 and 1.0. When n = 0, the disc becomes a homogeneous isotropic material. Tangential and radial stress distributions and displacements on the disc are investigated by taking different values of gradient parameters n and it is found that the stresses and displacements obtained from the analytical and numerical solutions are in good agreement. Radial stress σ_r and tangential stress σ_θ are varying in the radial direction of the disc depending on the power law function for elasticity modulus and mass density. Accordingly, radial stresses are zero at the inner and outer surfaces but they are of higher values at the interior parts of the discs and get lower values for n = 1.0 when compared with the results for n = 0 and n = 0.5. As for tangential stresses, they are higher at the inner surface for n = 0 and n = 0.5 than at the outer surface. Finally, a homogenous tangential stress distribution and the lowest radial stresses along the radius of a rotating disc are approximately obtained for the gradient parameter n = 1.0 compared with the homogeneous, isotropic case n = 0. The radial displacements increase gradually with a parallel curve with increasing the gradient parameter n. As a result of decreasing the tangential stresses, rotating capacity of the disc is increased nearly twice as much. This means that a disc made of FGMs has the capability of higher angular rotations compared with the homogeneous isotropic disc.

Callioglu [7] presented an analytical solution for thermo-elasticity equilibrium equations of a thin axisymmetric rotating disc made of FGM. Results for the stress and displacement along the radius were plotted related to internal and external pressure, centrifugal force and temperature. Power law distribution for functional gradation and infinitesimal deformation theory of elasticity were used in the solution technique. In the presence of internal or external pressure in a disc, the radial stress values were equal to internal or external pressure at the inner and outer surfaces. the normalized radial stresses at the inner section increase in a disc due to internal pressure (D1) or decrease more in a disc due to external pressure (D2) when the grading parameter n, was increased. The absolute maximum tangential stresses arise at the internal edge, and the normalized tangential stresses in D2 were found to be advanced than those of D1. The normalized radial displacements in D2 were noted to be greater than those of D1. The normalized radial and tangential stresses and radial displacements in a disc due to centrifugal force (D3) were increased with increasing grading parameter n and the normalized tangential stress components at the inside edge were found to be higher than those at the outer edge. The

normalized radial displacements at the outer surface were greater than those at the inner surface and by increasing the value of n, the values increase more, parallelly. The normalized radial stress components in a disc related to steady state temperature distribution (D4) were of the absolute maximum values at the inner segment. The normalized tangential stress components were found to be the highest at the inner surface but lowest at the outer surface for grading parameter value $n = -0.5$. They started decreasing at the inner surface whereas increase at the outer surface with increasing value of n. The radial displacements at the outer surface were also higher than those at the inner surface. From the results, it was concluded that the grading indexes play a significant role in determining the thermo mechanical comebacks of FG disc and in optimal design of these structures.

Damircheli*et al*. [11] carried out radial and hoop thermal and mechanical stress analysis of a rotating disk made of FGM with variable thickness by using finite element method (FEM) in two models of geometry and boundary conditions. It was hypothetical that the material properties, such as elastic modulus, Poisson's ratio and thermal expansion coefficient, were considered to vary using a power law function in the radial direction. Two geometrical models including thermal stress named as model-A and mechanical stress named as model-B were taken. Temperature distribution was as second order variation, whereas the material properties vary by a power law function in the radial track of the disk. In model-A, it was found that there exists no pressure in both external and internal layers, and there was a temperature circulation considered as a second order function in the radial direction of the rotating disk. The temperature dependency of the material properties was considered. In model-B, there was a constant pressure only on the internal layer of the disk without temperature distribution but on the other hand with different types of surface profiles. Validation and convergence was checked and good agreement was observed with other literature.

Gupta *et al*.[22]In this paper**,** an analytical analysis was carried out by the author on composite rotating disk with thickness variation in the presence of residual stresses. Shelby law & Hoffman yield criterion was used. Results were attained by using a computer program after doing a mathematical formulation for calculating radial and tangential strain rate for isotropic and anisotropic disks. It was observed that in the existence of residual stresses, the tangential stress and the radial stress does not vary much for an isotropic and anisotropic disk from inner to outer

radius. In fact there was a little difference in both the disks for tangential and radial stresses. Tangential stress first increased and then decreased while the radial stress at inner & outer radius increases first and then decreases and was extreme at the central radius. Tangential strain rate were also pointedly fluctuating i.e. greater at the inner & lower at the outer radius. This variation was supreme for isotropic and anisotropic with & without residual stresses.

Sharma *et al.*[9] used finite element method for stress and strain analysis of rotating FGM thermo elastic disk. It was determined that the stress, strain and displacement of FGM circular disk for fixed angular velocity get significantly modified due to uniform temperature variation, logarithmic thermal changes and non-heat conducting (isentropic) conditions. It was observed that the thermo elastic field in an FGM disk could be modeled and optimized by controlling thermal variations, radial thickness and temperature difference at inner and outer surfaces of the disk.

Peng*et al.* [24] executed an elastic analysis on a rotating sandwich solid disk which was composed of 3-parts or 3-layered provided additionally these layers were perfectly-bonded composites. The central and outer regions of the solid disk were made up of two homogeneous different materials whereas the middle region is a transition zone made up of functionally graded materials FGM. In the paper, two cases were measured. The first one in which the central region of FGM, composition varied according with power-law gradient and some equations for full elastic fields were derived. The second one is constituted with FGM with some radial non-homogeneity, for which an analytic approach is proposed to lessening the problem into a Fredholm integral equation. The results found from the second case were authenticated by comparing with the numerical results of the elastic fields with the precise ones for the case of power-law gradient. This presented the effects of the gradient, width variation of the FGM, and rotational velocity on the dispersal of the radial and hoop stresses for a rotating composite disk made of two constituents aluminum and zirconia. The method presented in this paper may be helpful for engineering designers in selecting suitable gradients and materials to acquire the best state of a rotating functionally graded disk.

CHAPTER 3

PROBLEM FORMULATION

3.1 RESEARCH GAPS

From the investigated literature it is summarized that the distribution of radial and tangential stresses and strain-rates in the rotating disc made up of composite materials under mechanical loading are affected by varying the values of stress exponent '*n*'. From the literature it is observed that various scholars used the particular values of stress exponent as *n*=3,5 or 8 for stress strain analysis and presented their results.

3.2 PROBLEMDESCRIPTION

So by extending the work performed formerly, it is decided to carry out stress strain analysis in rotating FGM disc by using the value of *n* = 3, 5, 8 and present the results for stresses and strain rates by taking different values of stress exponent and thereby reaching at some important conclusions.

For the above problem the material of the rotating disc is to be taken as Aluminum reinforced with silicon carbide i.e. Al–$SiC_{p.}$

The following well-documented creep law [19] will be used

$$\dot{\bar{\varepsilon}} = [M(\bar{\sigma} - \sigma_0)]^n. \quad . \quad . \quad . \quad . \quad . \quad . (3.1)$$

Where $M = \frac{1}{E}(A' exp \frac{-Q}{RT})^{1/n}$

where the symbols $\dot{\bar{\varepsilon}}$, $\bar{\sigma}$, σ_o,A',n, *Q, E, R* and *T* denote respectively the effective strain rate, effective stress, threshold stress, structure-dependent parameter, true stress exponent, true activation energy, temperature- dependent Young's modulus, gas constant, and operating temperature. M and σ_0 appearing in equation are the creep parameters describing steady state creep behavior, and are dependent on the material.

3.3 METHODOLOGY ADOPTED

1. Mathematical formulation has been developed for the problem to obtain creep rates in a rotating disc of functionally graded material and equations have been solved for creep strains and stresses.
2. A computer code is prepared based on the mathematical formulation developed to obtain the distribution of stresses and steady state creep rates in the rotating disc.
3. Obtained results are analyzed and compared with the results available in literature to draw some important inferences.

3.4 ASSUPTIONS TAKEN

a) The material of the disc is incompressible, isotropic, and possesses uniform distribution of SiC_p in the aluminium matrix.
b) Stresses at any point in the disc remain constant with time, i.e. the steady state condition is assumed.
c) Elastic deformations in the disc are small and neglected when compared with creep deformations.
d) The thickness of the disc is very small compared with its diameter; therefore the axial stress is assumed to be zero throughout the disc.

CHAPTER 4

MATHEMATICAL FORMULATION

In this chapter an estimation of steady state creep parameters of a rotating FG disc having constant thickness are computed. The creep behavior of the disc material has been described by Sherby's constitutive model. The model developed has been used to determine the stress and strain rate distributions. The material of the disc is anticipated to yield following Tresca's failure criterion.

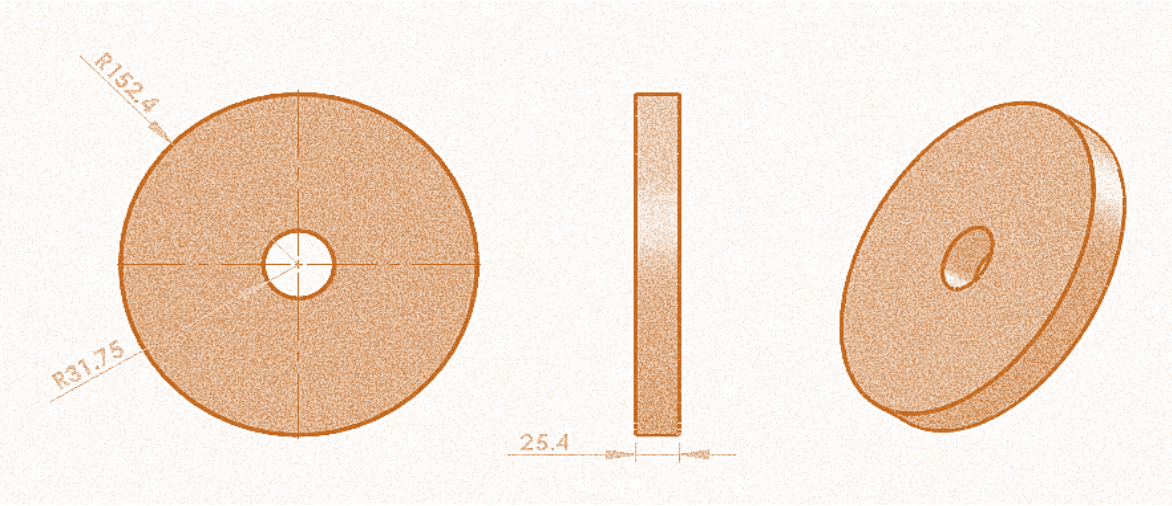

Figure4.1 Schematic diagram of rotating disc geometry

The inner and outer radii *a* and *b* are assumed as 31.75mm and 152.4mm, respectively whereas the thickness is taken as 25.4 mm. The thickness is uniform throughout the disc as shown in fig 4.1

$$\text{i.e. } h(r) = t = 25.4\text{mm} \quad . \quad . \quad . \quad . \quad . \quad . \quad . \quad . \quad . \quad . \quad . \quad . \quad . \quad . \quad . \quad (4.1)$$

4.1 DISTRIBUTION OF REINFORCEMENT: The distribution of reinforcement of SiC in the FGM disc decreases linearly from inner towards the outer radius. Therefore, the density and the creep constant will also vary with radial distance. The volume % of SiC, *V(r)* at any radius '*r*'[16] is given by:

$$V(r) = V_{max} - \frac{(r-a)}{(b-a)}(V_{max} - V_{min}). \quad . \quad . \quad . \quad . \quad . \quad . \quad . \quad . \quad . \quad . \quad . \quad (4.2)$$

$$V(r) = \delta_1 - \delta_2 r$$

Where $\delta_1 = (V_{max} + a\delta_2)$

$$\delta_2 = \frac{V_{max} - V_{max}}{(b-a)}$$

$V_{max}$and V_{min} are the maximum and minimum SiC_p contents at the inner and outer radii.

According the rule of mixture, the density ρ*(r)* of the FGM disc at any radius 'r' may be given as

$$\rho(r) = \frac{[100 - V(r)]\rho_m + V(r).\rho_d}{100}$$

$$\rho(r) = \rho_m + \frac{(\rho_d - \rho_m).V(r)}{100} \quad . \quad . \quad . \quad . \quad . \quad . \quad . \quad . \quad . \quad . (4.3)$$

Where $\rho_d = 2698.9\ kg/m^3$

$$\rho_m = 3210\ kg/m^3$$

Substituting *V(r)* from Eq. (4.2) into Eq. (4.3)

$$\rho(r) = \rho_m + \frac{(\rho_d - \rho_m)}{100}(\delta_1 - \delta_2 r)$$

$$\rho(r) = \rho_m + \frac{(\rho_d.\delta_1 - \rho_m.\delta_1 - \rho_d.\delta_2.r + \rho_m.\delta_2.r)}{100}$$

$$\rho(r) = \rho_m + \frac{(\rho_d - \rho_m).\delta_1}{100} - \frac{(\rho_d - \rho_m).\delta_2.r}{100}$$

$$\rho(r) = A_\rho - B_\rho.r \quad . \quad . \quad . \quad . \quad . \quad . \quad . \quad . \quad . \quad . \quad . \quad . \quad . \quad . \quad . \quad . \quad . \quad . (4.4)$$

Where $A_\rho = \rho_m + \frac{(\rho_d - \rho_m).\delta_1}{100}$

and$B_\rho = \frac{(\rho_d - \rho_m).\delta_2.r}{100}$

The average particle content in the disc (V_{avg}) can be expressed as

$$V_{avg} = \frac{\int_a^b 2\pi rt.V(r).dr}{\pi(b^2-a^2).t} \quad \ldots\ldots\ldots\ldots\ldots\ldots \quad (4.5)$$

Substituting t and $V(r)$ from Eq. (4.1) and Eq. (4.2) into above Eq. the minimum SiC_pContent,V_{min} in the disc may be obtained as

$$V_{min} = \frac{3V_{avg}(1-\alpha^2)(1-\alpha) - V_{max}(1-3\alpha^2+2\alpha^3)}{(2-3\alpha+\alpha^3)} \quad \ldots\ldots\ldots\ldots \quad (4.6)$$

Where $where\ \alpha = \frac{a}{b}$

4.2 ESTIMATION OF CREEP PARAMETERS

In the current investigation, the material of the rotating disc, i.e. Al–SiC_p, is assumed to undergo steady state creep following the well-documented creep law given by,

$$\dot{\bar{\varepsilon}} = \mathrm{A}'\left(\frac{(\bar{\sigma}-\sigma_0(r))}{\mathrm{E}}\right)^n exp\left(\frac{-Q}{RT}\right)$$

where the symbols$\dot{\bar{\varepsilon}}$, $\bar{\sigma}$, σ_o,A',n, Q, E, R, and T denote respectively the effective strain rate, effective stress, threshold stress, structure-dependent parameter, true stress exponent, true activation energy, temperature- dependent Young's modulus, gas constant, and operating temperature.

Creep Law is $\dot{\bar{\varepsilon}} = [M(r)(\bar{\sigma}-\sigma_0(r))]^n \quad \ldots\ldots\ldots\ldots \quad (4.7)$

where$M(r) = \frac{1}{E}(A' exp\frac{-Q}{RT})^{1/n}$

M and σ_0 appearing in equation are the creep parameters describing steady state creep behavior, and are dependent on the material [4] as follows

$$M(r) = 0.0288 - \frac{0.0088}{P} - \frac{14.0267}{T} - \frac{0.0322}{V(r)} \quad \ldots\ldots\ldots\ldots \quad (4.8)$$

$$\sigma_0(r) = -0.084.P - 0.0232.T + 1.185.V(r) + 22.207 \quad \ldots\ldots\ldots\ldots \quad (4.9)$$

P=Dispersoid Size,

T=Temperature,

V(r) =Content of dispersoid

The general constitutive equations for creep in an isotropic composite disc under biaxial state of stress is taken as the following form when the reference frame is along the principal directions of r, θ, and z [19].

$$\dot{\varepsilon}_r = \frac{\dot{\bar{\varepsilon}}}{2\bar{\sigma}}(2\sigma_r - \sigma_\theta) \quad . \quad . \quad . \quad . \quad . \quad . \quad . \quad . \quad . \quad . \quad . \quad . \quad (4.10)$$

$$\dot{\varepsilon}_\theta = \frac{\dot{\bar{\varepsilon}}}{2\bar{\sigma}}(2\sigma_\theta - \sigma_r) \quad . \quad . \quad . \quad . \quad . \quad . \quad . \quad . \quad . \quad . \quad . \quad . \quad (4.11)$$

$$\dot{\varepsilon}_z = \frac{\dot{\bar{\varepsilon}}}{2\bar{\sigma}}(-\sigma_r - \sigma_\theta) \quad . \quad . \quad . \quad . \quad . \quad . \quad . \quad . \quad . \quad . \quad . \quad . \quad (4.12)$$

The current study assumes that the disc material is isotropic and creeps according to the Tresca yield criterion. Therefore, the effective stress,$\bar{\sigma}$ in a rotating disc under biaxial state of stress (i.e. σ_z=*0*) is given by Using Tresca yield criterion

$$\bar{\boldsymbol{\sigma}} = \boldsymbol{\sigma_\theta}$$

Putting the values of $\dot{\bar{\varepsilon}}$ and $\sigma_\theta$in equation (4.10)

$$\dot{\varepsilon}_r = \frac{du_r}{dr} = \frac{[M(r)(\bar{\sigma} - \sigma_0)]^n}{2\sigma_\theta}(2\sigma_r - \sigma_\theta)$$

$$\dot{\varepsilon}_r = \frac{d\dot{u}_r}{dr} = \frac{(2x-1)}{2}[M(r)(\bar{\sigma} - \sigma_0)]^n \quad . \quad . \quad . \quad . \quad . \quad . \quad . \quad . \quad . \quad . \quad . \quad (4.13)$$

$$where\ \frac{\sigma_r}{\sigma_\theta} = x$$

Similarlily putting the values of $\dot{\bar{\varepsilon}}$ and $\sigma_\theta$in equation (4.11)

$$\dot{\varepsilon}_\theta = \frac{\dot{u}_r}{r} = \frac{[M(r)(\bar{\sigma} - \sigma_0)]^n}{2\sigma_\theta}(2\sigma_\theta - \sigma_r)$$

$$\dot{\varepsilon}_\theta = \frac{\dot{u}_r}{r} = \frac{(2-x)}{2}[M(r)(\bar{\sigma} - \sigma_0)]^n \quad . \quad . \quad . \quad . \quad . \quad . \quad . \quad (4.14)$$

Dividing Eq. (4.13) by Eq. (4.14)

$$\frac{d\dot{u}_r}{dr} \cdot \frac{r}{\dot{u}_r} = \frac{(2x-1)}{(2-x)}$$

$$\frac{d\dot{u}_r}{\dot{u}_r} = \frac{\emptyset(r)}{r}\, dr \qquad \text{Where } \emptyset(r) = \frac{(2x-1)}{(2-x)}$$

Integrating above Eq. from limits *a* to *r*,

$$\int_a^r \frac{d\dot{u}_r}{dr} = \int_a^r \frac{\emptyset(r)}{r}\, dr$$

$$\log \dot{u}_r \,|_a^r = \int_a^r \frac{\emptyset(\mathrm{r})}{r}\, dr$$

$$(\log \dot{u}_r - \log \dot{u}_a) = \int_a^r \frac{\emptyset(r)}{r}\, dr$$

$$log \frac{\dot{u}_r}{\dot{u}_a} = \int_a^r \frac{\emptyset(\mathrm{r})}{r}\, dr$$

Now taking antilog on both sides

$$\frac{\dot{u}_r}{\dot{u}_a} = exp\left[\int_a^r \frac{\emptyset(\mathrm{r})}{r}\, dr\right]$$

$$\dot{u}_r = \dot{u}_a exp\left[\int_a^r \frac{\emptyset(\mathrm{r})}{r}\, dr\right] \quad . \; . \; . \; . \; . \; . \; . \; . \; . (4.15)$$

Substituting the value of $\dot{u}_r$ in Eq. (4.14)

$$\frac{\dot{u}_a}{r} . exp\left[\int_a^r \frac{\emptyset(\mathrm{r})}{r}\, dr\right] = \frac{(2-x)}{2}[M(r)(\overline{\sigma} - \sigma_0)]^n$$

$$\frac{\dot{u}_a}{r} . \frac{2}{(2-x)} . exp\left[\int_a^r \frac{\emptyset(\mathrm{r})}{r}\, dr\right] = [M(r)(\overline{\sigma} - \sigma_0)]^n$$

$$\dot{u}_r{}^{1/n} \psi^{1/n} = [M(r)(\overline{\sigma} - \sigma_0)]^n$$

$$\text{Where } \psi(\mathrm{r}) = \frac{1}{\mathrm{r}} \frac{2}{(2-x)} . exp\left[\int_a^r \frac{\emptyset(\mathrm{r})}{r}\, dr\right]$$

$$\frac{[\dot{u}_r \psi(r)]^{\frac{1}{n}}}{M(r)} = (\overline{\sigma} - \sigma_0)$$

$$\frac{\dot{u}_r{}^{1/n} \psi^{1/n}}{M(r)} = (\overline{\sigma} - \sigma_0)$$

$$\overline{\sigma} = \frac{\dot{u}_r{}^{1/n} \psi^{1/n}}{M(r)} + \sigma_0(r)$$

But according to Tresca yield theory, $\overline{\boldsymbol{\sigma}} = \boldsymbol{\sigma_\theta}$

So the above expression becomes $\sigma_\theta = \frac{{ui_r}^{1/n}\psi^{1/n}}{M(r)} + \sigma_0(r)$ . . . . . (4.16)

The equilibrium equation of rotating disc of uniform thickness is given by [14]

$$\frac{d}{dr}(r.\sigma_r) - \sigma_\theta + \rho(r)\omega^2 r^2 = 0 \quad . \ . \ . \ . \ . \ . \ . \ . \ . \ . \ . \ (4.17)$$

$$d(r.\sigma_r) - \sigma_\theta dr + \rho(r)\omega^2 r^2 dr = 0$$

Integrating it from limits *a* to *b*,

$$\int_a^b d(r.\sigma_r) - \int_a^b \sigma_\theta dr + \int_a^b \rho(r)\omega^2 r^2 dr = 0$$

$$\int_a^b \sigma_\theta dr = \int_a^b d(r.\sigma_r) + \omega^2 \int_a^b \rho(r) r^2 dr$$

$$\int_a^b \sigma_\theta dr = r.\sigma_r|_a^b + \omega^2 \int_a^b (A_\rho - B_\rho.r) r^2 dr$$

$$\int_a^b \sigma_\theta dr = (b.\sigma_r - a.\sigma_r) + \omega^2 \left[\int_a^b A_\rho.r dr - \int_a^b B_\rho.r^3 dr\right]$$

Now applying the boundary conditions are

$$\sigma_r = 0 \ at \ r = a$$

$$\sigma_r = 0 \ at \ r = b$$

$$\int_a^b \sigma_\theta dr = \omega^2 \left[\frac{A_\rho(b^3 - a^3)}{3} - \frac{B_\rho(b^4 - a^4)}{4}\right]$$

Dividing above Eq. by (b-a) we get

$$\sigma_{\theta avg} = \frac{\int_a^b \sigma_\theta dr}{b - a}$$

$$\sigma_{\theta avg} = \frac{\omega^2}{b-a}\left[\frac{A_\rho(b^3 - a^3)}{3} - \frac{B_\rho(b^4 - a^4)}{4}\right] \quad . \ . \ . \ . \ . \ . \ . \ . (4.18)$$

From Eq. (4.16) $\sigma_\theta = \frac{{ui_r}^{1/n}\psi^{1/n}}{M(r)} + \sigma_0(r)$

Multiplying the above Eq. by *dr* both sides and integrating it from limits *a* to *b*,

$$\int_a^b \sigma_\theta dr = \int_a^b \frac{{ui_r}^{1/n}\psi^{1/n}}{M(r)} dr + \int_a^b \sigma_0 dr$$

$$\int_a^b \sigma_\theta dr = {ui_r}^{1/n} \int_a^b \frac{\psi^{1/n}}{M(r)} dr + \int_a^b \sigma_0 dr$$

$$\int_a^b \sigma_\theta dr - \int_a^b \sigma_0 dr = \dot{u_r}^{1/n} \int_a^b \frac{\psi^{1/n}}{M(r)} dr$$

$$\dot{u_r}^{1/n} = \frac{\int_a^b \sigma_\theta dr - \int_a^b \sigma_0 dr}{\int_a^b \frac{\psi^{1/n}}{M(r)} dr} \quad \ldots\ldots\ldots\ldots \quad (4.19)$$

Substituting the value of $\dot{u_r}^{1/n}$ in Eq. (16), then the resulting equation becomes

$$\sigma_\theta = \left(\frac{\int_a^b \sigma_\theta dr - \int_a^b \sigma_0 dr}{\int_a^b \frac{\psi^{1/n}}{M(r)} dr} \right) \frac{\psi^{1/n}}{M(r)} + \sigma_0(r) \quad \ldots\ldots\ldots \quad (4.20)$$

The equilibrium equation of rotating disc of uniform thickness is given by

$$\frac{d}{dr}(r.\sigma_r) - \sigma_\theta + \rho(r)\omega^2 r^2 = 0$$

$$d(r.\sigma_r) - \sigma_\theta dr + \rho(r)\omega^2 r^2 dr = 0$$

Integrating from limits *a* to *r*,

$$\int_a^r d(r.\sigma_r) - \int_a^r \sigma_\theta dr + \int_a^r \rho(r)\omega^2 r^2 dr = 0$$

$$\int_a^r d(r.\sigma_r) - \int_a^r \sigma_\theta dr + \int_a^r \rho(r)\omega^2 r^2 dr = 0$$

$$r.\sigma_r|_a^r = \int_a^r \sigma_\theta dr + \omega^2 \int_a^r (A_\rho - B_\rho.r) r^2 dr$$

$$(r.\sigma_r - a.\sigma_r) = \int_a^r \sigma_\theta dr + \omega^2 \left[\frac{A_\rho(b^3 - a^3)}{3} - \frac{B_\rho(b^4 - a^4)}{4} \right]$$

Applying the boundary conditions,

$$\sigma_r = \frac{1}{r}\left[\int_a^r \sigma_\theta dr + \omega^2 \left(\frac{A_\rho(b^3 - a^3)}{3} - \frac{B_\rho(b^4 - a^4)}{4} \right) \right] \quad \ldots\ldots\ldots \quad (4.21)$$

CHAPTER 5

RESULTS AND DISCUSSIONS

On the basis of mathematical formulation, a computer program has been developed in C++.To find out the distribution of stresses & steady state creep rates, the procedure adopted is shown by the flow chart (Figure 5.1) in the rotating disk for the different values of stress exponent *n.* Since it is an iterative process, to make the convergence fast, 75 % of the value of σ_θ from the current iteration obtained has been mixed with 25% of the value of σ_θ of previous iteration.

5.1 VALIDATION:

Before discussing the present results, it is foremost necessary to check the correctness of the present analysis done and the computer program developed. To verify these results, the program has been run for steel disc parameters detailed in the Table 5.1 (Wahl *et al*.)[1] and are compared for tangential stresses. The following data for steel disk is taken for validation

Table 5.1. Parameters and operating conditions for steel disc

PARAMETERS FOR STEEL DISK	VALUE
Density of the disc material ρ (kg/m^3)	7823.18
Disk radii	
Inner Radius, *a* (mm)	31.75
Outer Radius *b* (mm)	152.40
Stress exponent, *n*	5
CREEP PARAMETERS	
M(r) (s$^{-1/5}$/MPa)	2.36087 x 10^{-4}
$\sigma_0(r)$ (MPa)	-59.03
OPERATING CONDITIONS	
Disk RPM	15,000
Working temperature (K)	810.78
Creep period (hours)	180

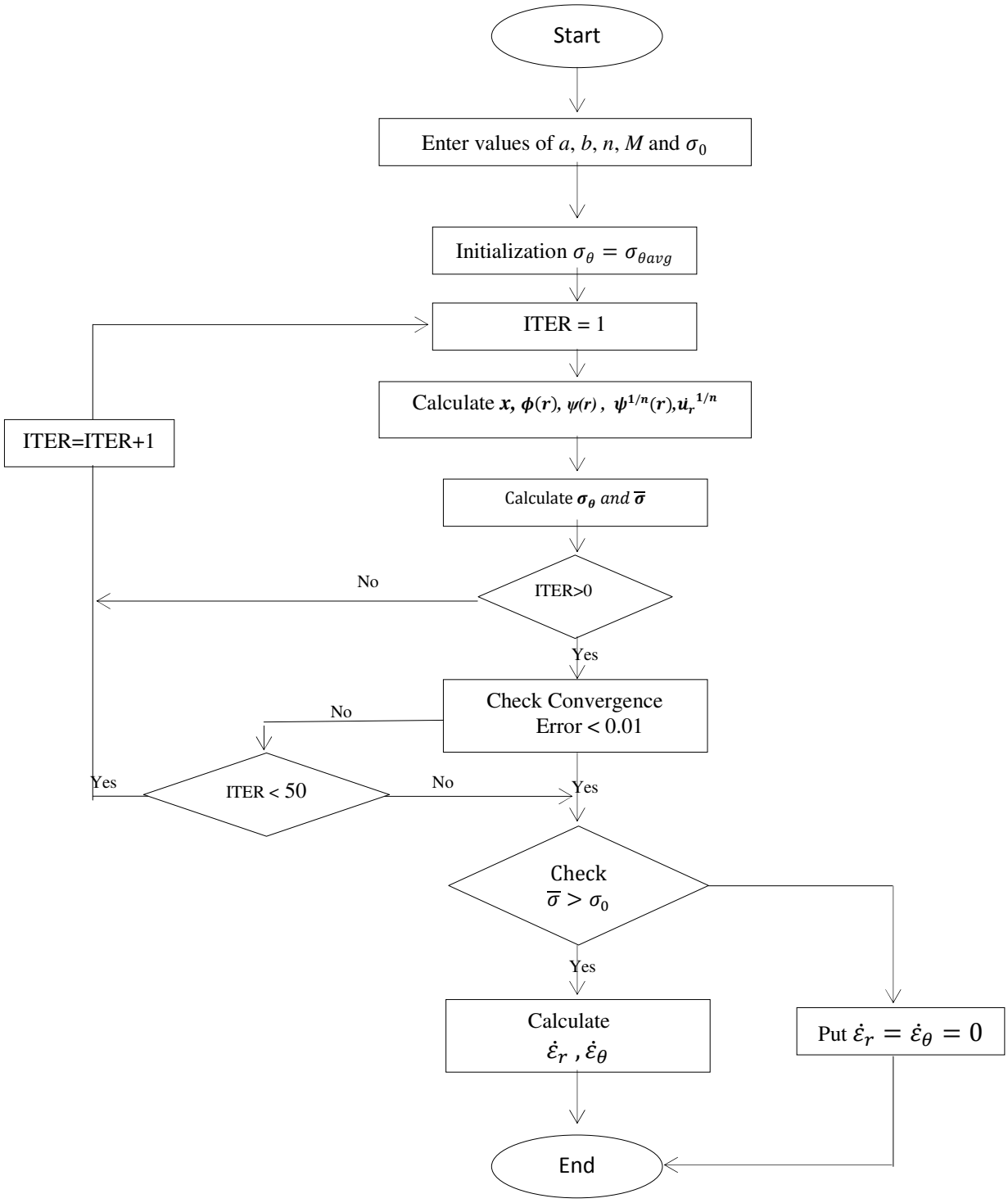

Figure 5.1 Numerical Computation Scheme

To obtain the creep parameter M and σ_0 given in table 1, for steel disk, following equation

$$\dot{\bar{\varepsilon}} = [M(\bar{\sigma} - \sigma_0)]^n \quad . \quad . \quad . \quad . \quad . \quad . \quad . \quad . \quad . \quad . \quad . \quad (5.1)$$

is integrated to obtain, $\dot{\bar{\varepsilon}} = [M(\bar{\sigma} - \sigma_0)]^n \int_0^t f(t)dt \quad . \quad . \quad . \quad . \quad . \quad . \quad (5.2)$

Where $\dot{\bar{\varepsilon}}$ is the effective strain and *f(t)* is a function of time *t*. As per the study done by Wahl *etal*.[1] the function *f(t)* is assumed to be unity. In that experimental study it was presented that the average strain after 180 hours for mean true stress $\bar{\sigma}$ is 25150 psi and 29450 psi are 0.0109 and 0.0029 in/in respectively. By setting these values in equation 5.2, the value of creep parameter M & σ_0 as 2.36087 x 10^{-4} and -59.03 MPa. The parameters reported in Table 5.1 have been used in the current computer C++ code to achieve the results for radial & tangential stresses. The figure 5.2 shows a good agreement between the results from present study and the experimental results given by Wahl *et al.*[1].

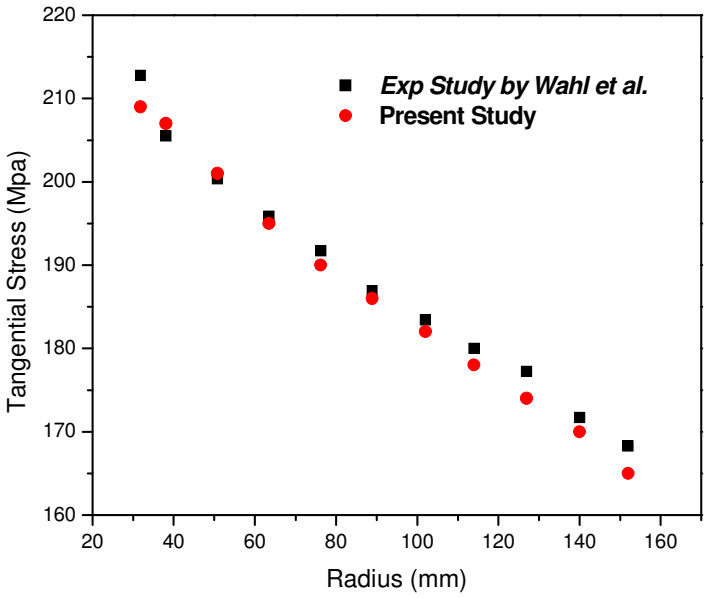

Figure 5.2 Comparison of experimental and present results

5.2 EFFECT OF STRESS EXPONENT ON CREEP: The present results based on the mathematical formulation, the radial and tangential stresses and strains have been obtained and demonstrated in the form of graphs as shown in the coming section:

Fig. 5.3, 5.4, 5.5 and 5.6 shows the creep response of the FGM disc for the different values of stress exponent using 25% maximum volume, 20% average volume and 1.7μmas particle size of the reinforcement at a temperature of 623 K.

Table 5.2 Description of the rotating discs

Type of Disc	***Vmax %***	***Vavg %***	***Vmin %***	***Particle Size (P) (μm)***	***Stress Exponent (n)***	***Temperature T***
FGM	*25*	*20*	*16.7925*	*1.7*	*3* *5* *8*	*623 K*
FGM	*25*	*20*	*16.7925*	*1.7* *14.5* *45.9*	*5*	*623 K*
Non-FGM *FGM* *FGM*	*20* *25* *30*	*20* *20* *20*	*20* *16.7925* *13.5849*	*14.5*	*5*	*623 K*

Fig 5.3 & 5.4 shows the creep responses of the composite disc under the various values of stress exponent *n*. In fig 5.3, radial stress versus radius graph is plotted. It shows how the radial stress is distributed in the disk from inner towards the outer radius. It can be seen that the radial stress corresponds to *n*=3, is relatively higher over the entire disc, when compared with the values of stress exponent *n*=5 & *n*=8. The radial stress corresponds to *n*=8 is comparatively lower than those related to the other values. The maximum difference observed in radial stress for *n*=3 and *n*=8 is 3.2 MPa approximately at a radius of 72 mm lies near to the middle radius. As it is clear that the results of the radial stress for *n*=5 is always lies in between the values of *n*=3 and *n*=8.

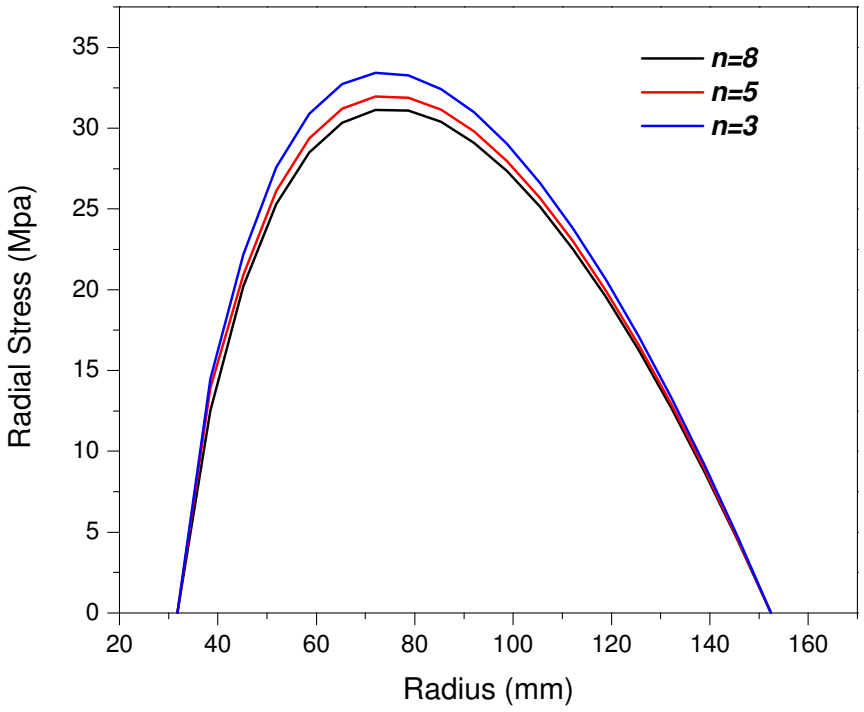

Figure 5.3 Effect of stress exponent on radial stress

In fig 5.4 tangential stresses versus radius graph is plotted. It shows how the tangential stress varies when one moves from inner towards the outer radius of the disc. It can be seen that the tangential stress corresponds to n=3, is relatively higher upto the middle radius of the disc as compared to the values of stress exponent n=5 and n=8. The trend of the variation is just opposite before the middle and after the middle radius. Over the entire disc the tangential stress based on n=5 lies between the resultant values based on n=3 and n=8. In the middle of the disc, someplace around a radial distance of 85mm, the tangential stress matching to various values of stress exponent n remains the same. The variation in tangential stress, corresponding to n=3 and n=8, noted at the internal radius of the disc is 10.7 MPa approximately and 7.4 Mpa approximately at the outside radius.

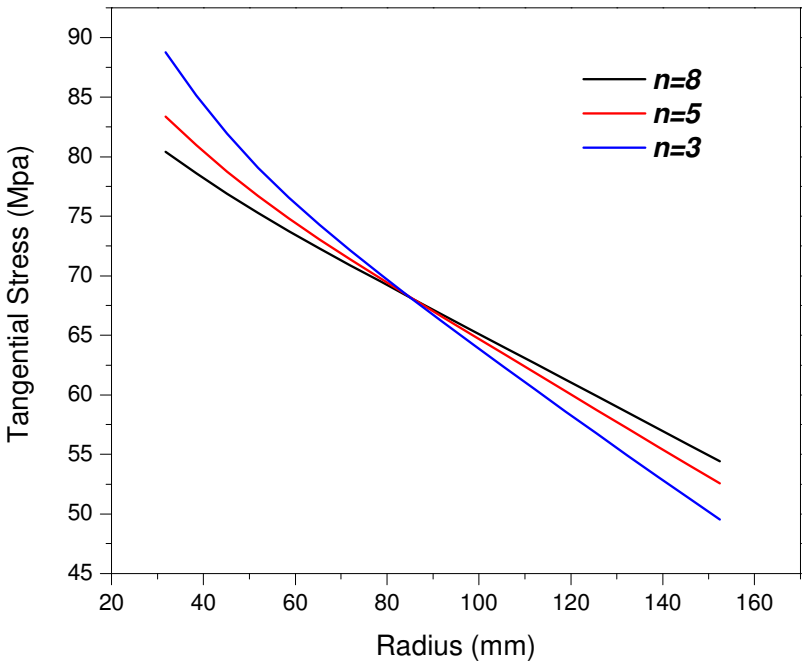

Figure 5.4 Effect of stress exponent on tangential stress

Fig. 5.5 & 5.6 shows the radial strain rates (compressive) and the tangential strain rates. Radial strain rates are considerably affected by changing the stress exponent. All over the disc, the radial strain rate based on n=8 is the maximum and that corresponding to n=3 is the lowest corresponding to n=5 remains in between the values observed for n=3 and n=8. The radial strain rate based on n=8 is higher by about two orders of magnitude compared with that corresponds to n=3.

The effect of stress exponent on tangential strain rate is also similar to those detected for radial strain rate in Fig. 5.5. and as shown in Fig. 5.6.

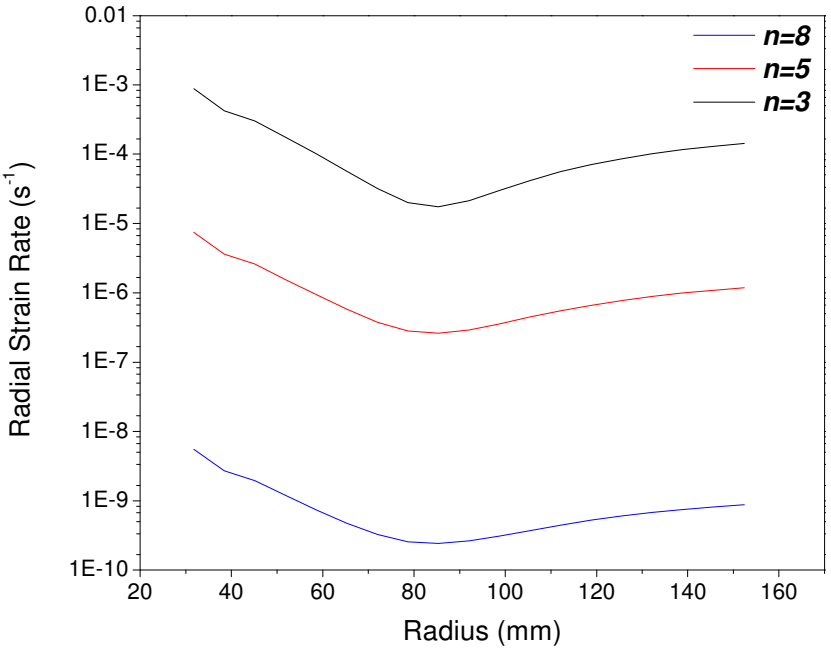

Figure 5.5 Effect of stress exponent on radial strain rate.

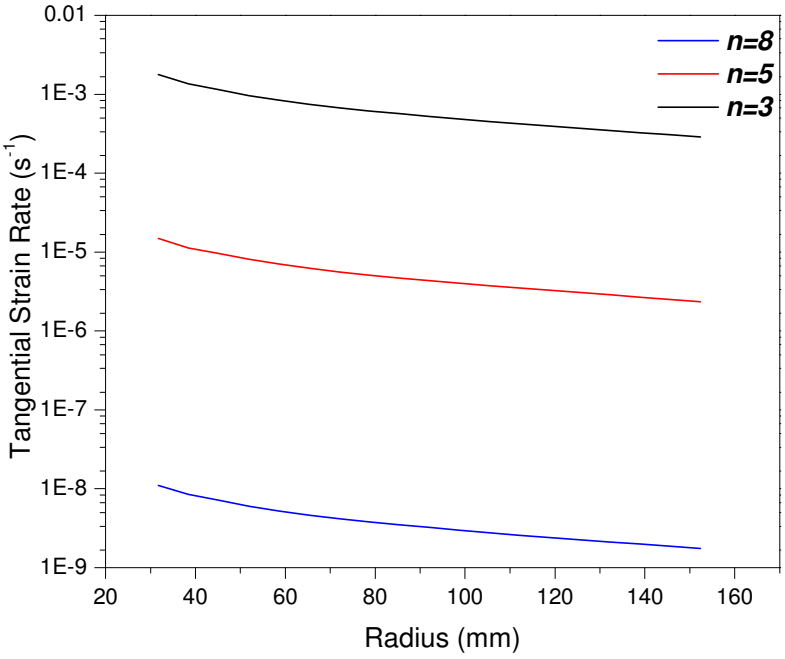

Figure 5.6 Effect of stress exponent on tangential strain rate

5.3 EFFECT OF DISPERSOIDSIZE ON CREEP

Fig. 5.7, 5.8, 5.9 and 5.10 shows the creep response of the FGM disc for the different values of dispersoid size by taking *P*=1.5*μm*, 14.5*μm* , 45.9*μm*by reinforcing with SiC of 25% maximum volume, 20% average volume and *n*=5as the stress exponent employing 623 K working temperature as shown in table 5.2. In fig 5.7, radial stress versus radius graph is plotted. It shows how the radial stress is distributed in the disk from inner towards the outer radius. From Fig. 5.7, it can be seen that the radial stress corresponds to *P=1.7μm*, is relatively higher over the entire disc, when compared with the values of particle content size *P=14.5μm& P=45.9 μm*. The radial stress corresponds to *P=1.7μm*is comparatively higher than those related to the other values. The maximum difference detected in radial stress for *P=1.7μm*and *P=14.5μm*is 0.874Mpa approximately at a radius of 72 mm lies near to the middle radius.

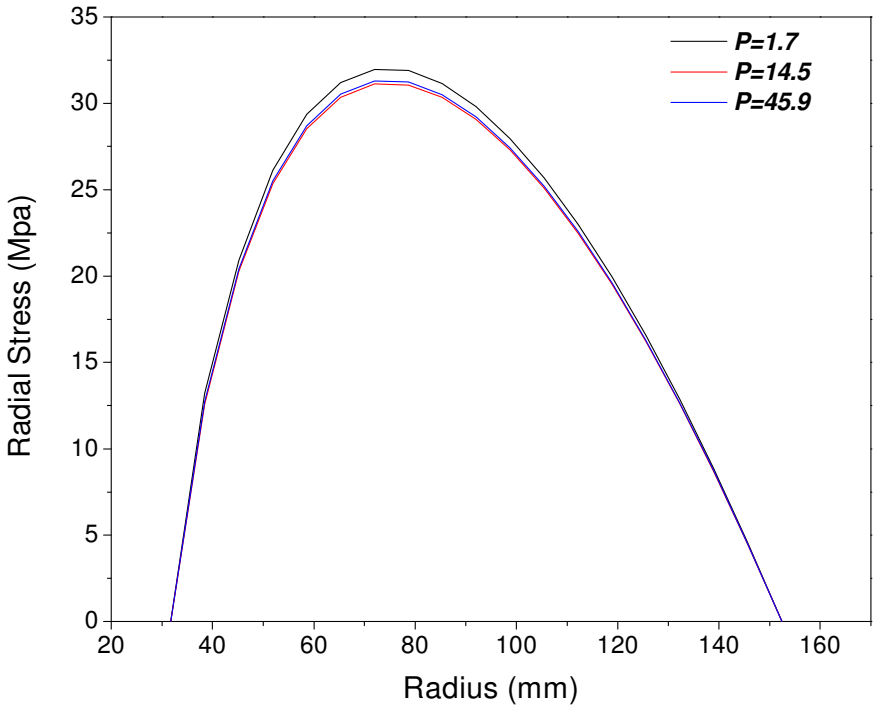

Figure 5.7 Effect of dispersoid size on radial stress

From Fig. 5.8, it can be seen that the tangential stress corresponds to *P=1.7μm*, is relatively higher upto the middle of the disc. As it is clear from the graph that the results of the tangential stress for *P=45.9μm* is always lies in between the values of *P=1.7μm* and *P=14.5μm*. The trend of the variation is reversed after the middle radius. In the middle of the disc, somewhere around a radial distance of 85mm, the tangential stress becomes same for all values of dispersoid size. The total variation in tangential stress, corresponding to *P=1.7μm*and *P=14.5μm*, noted at the internal radius of the disc is 1.939 MPa approximately and 2.083MPa approximately at the outside radius.

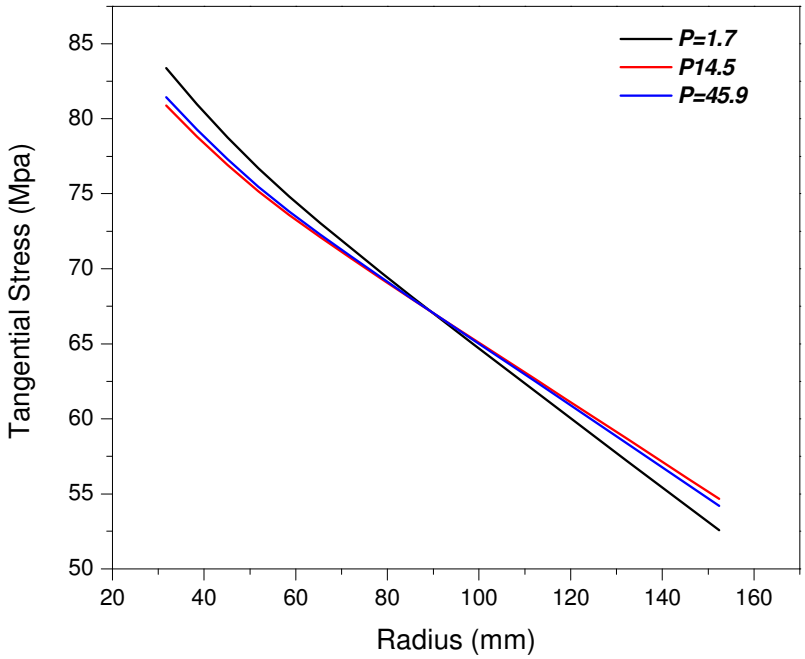

Fig. 5.8 Effect of dispersoid size on tangential stress

Fig. 5.9 & 5.10 shows the radial strain rates (compressive) and the tangential strain rates. As it is clear from the graphs that the radial strain rates are considerably affected by changing the dispersoid size *P*.

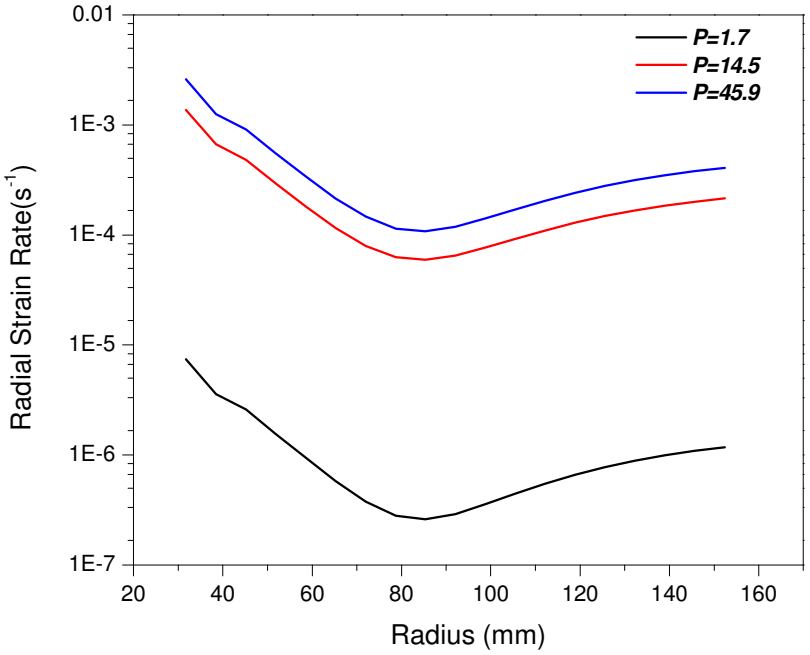

Fig. 5.9 Effect of dispersoid size on radial strain rate

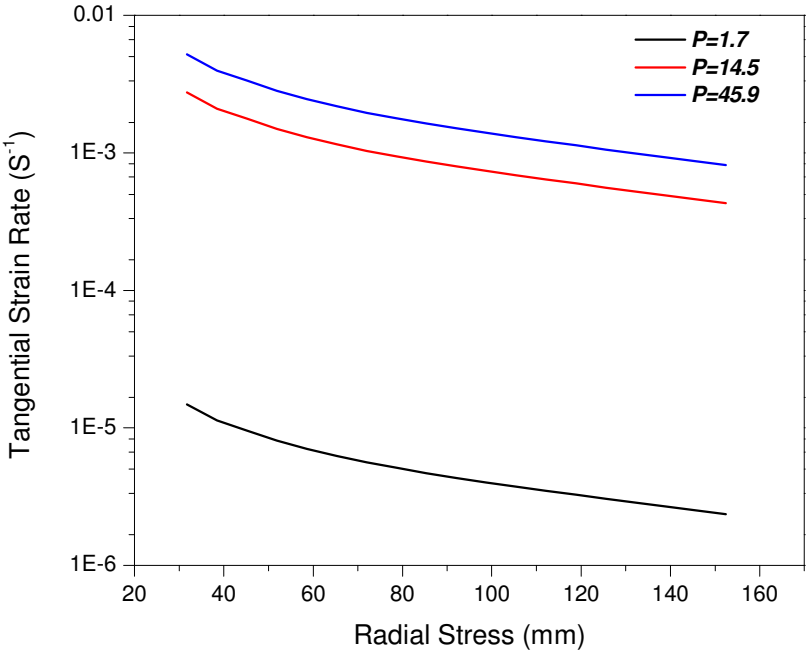

Figure 5.10 Effect of dispersoid size on tangential strain rate.

From results, it is concluded that the change in particle size of the reinforcement affects the tangential strain rate quite significantly. It is expected that the smaller size particles will be more in amount for the similar volume fraction and are capable to restrain creep flow more effectively. This is clearly evident from the figure that the creep rate at any radius is reduced by almost three orders of magnitude when the particle size decreases from 45.9 μm to 1.7 μm

5.4 EFFECT OF REINFORCEMENT VOLUME ON CREEP

Fig. 5.11, 5.12, 5.13 and 5.14 show the creep response of the FGM discussing different maximum and average volume combinations as shown in Table 5.2 and keeping stress exponent value n=5 under 623 K operating. From Fig. 5.11, it can be seen that the radial stress corresponds to Non-FGM disc i.e. uniform composite disc is relatively higher over the entire disc, when compared with the FGM disc. The maximum difference detected in radial stress for composite disc and FGM disc with 30% volume content is 4.191 MPa approximately at a radius of 72 mm lies near to the middle radius.

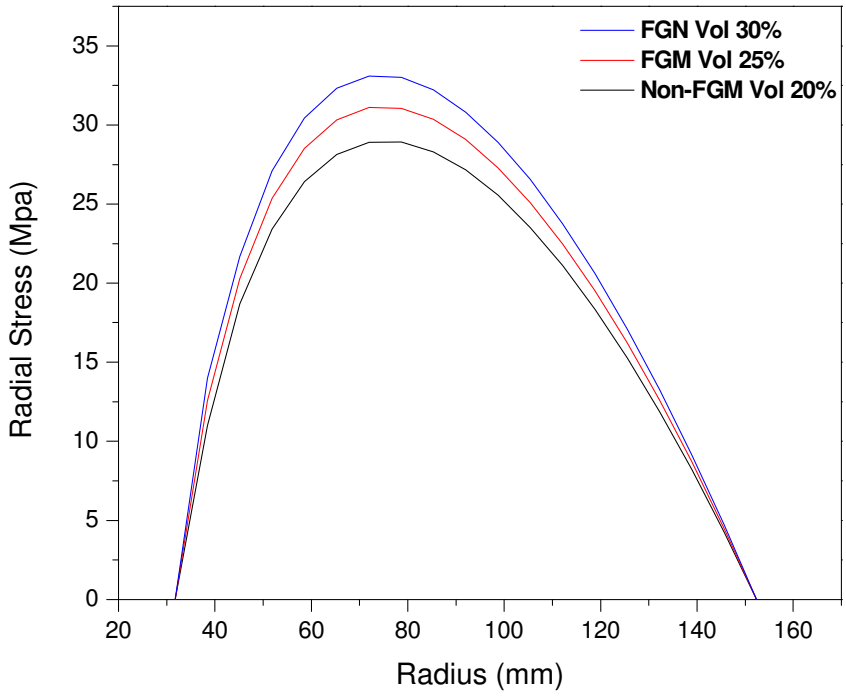

Fig. 5.11 Effect of reinforcement volume on radial stress

From Fig. 5.12, it can be realized that the tangential stress corresponds to a Non-FGM disc i.e. a composite disc is relatively lower over the entire disc when compared with the values of *FGM* discs. The trend of the variation is just opposite of that observed near the inner radius towards the outer radius. In the middle of the disc, somewhere around a radial distance of 85mm, the tangential stress matching to various discs remains the same. The maximum variation in tangential stress, of a uniform composite disc and a FGM disc with 30% volume content noted at the internal radius of the disc is 11.4MPa approximately and 12.4MPa approximately at the outside radius.

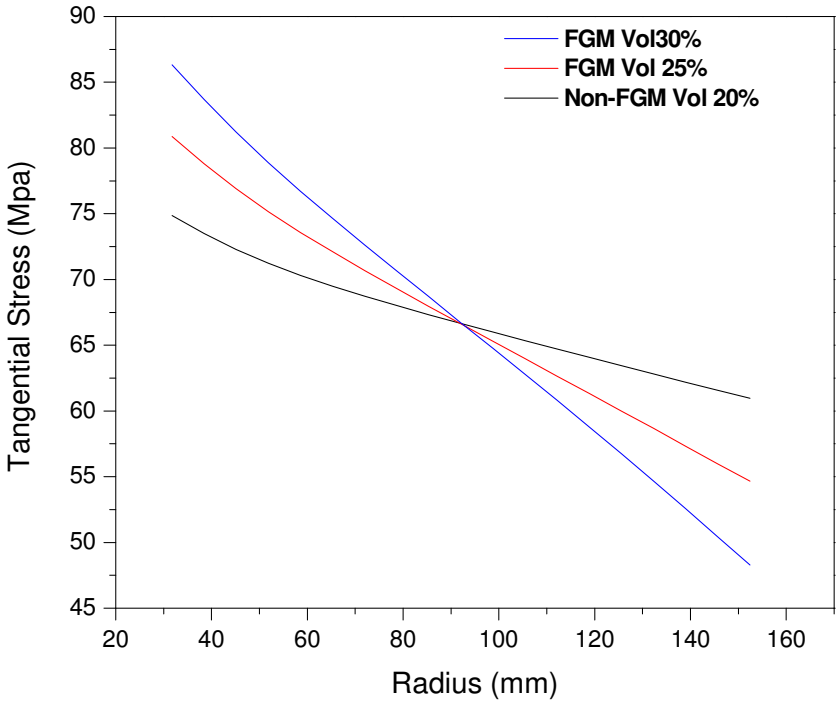

Figure 5.12 Effect of reinforcement volume on tangential stress

Fig. 5.13 & 5.14 shows the radial strain rates (compressive) and the tangential strain rates for FGM and Non-FGM discs. As it can be observed that the radial strain rates are considerably affected by changing the reinforcement volume.

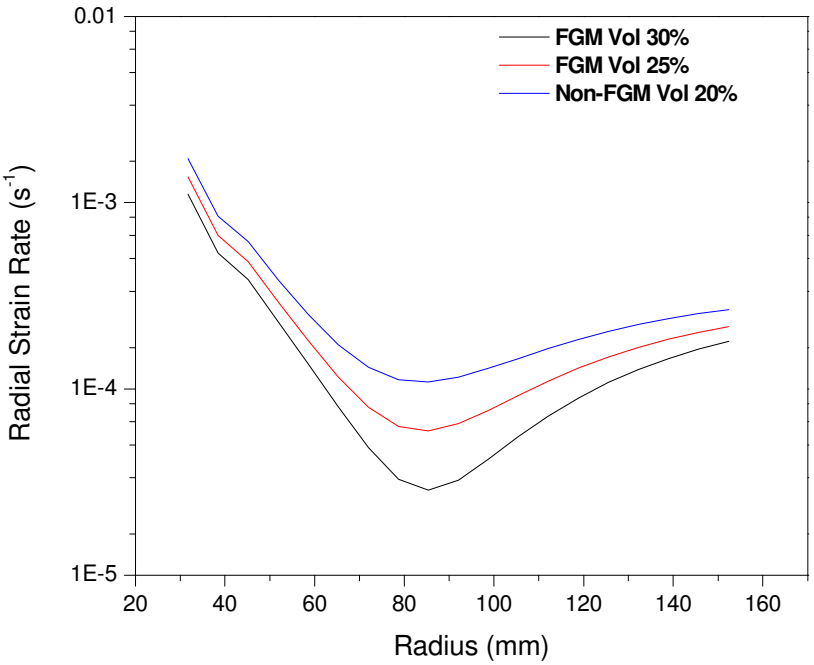

Fig. 5.13 Effect of reinforcement volume on radial strain rate

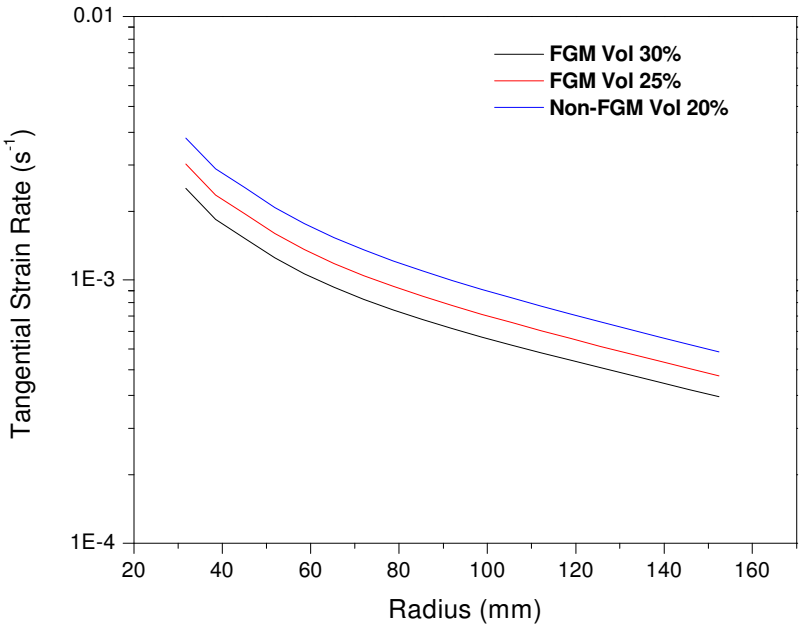

Fig. 5.14 Effect of reinforcement volume on tangential strain rate

From the results it is determined that the change in the reinforcement volume of SiC affects the tangential strain rate quite significantly. It was observed that the trend of radial and tangential stresses is similar to the previous cases. Tangential stress is higher for FGM disc when 30% maximum volume of SiC is reinforced in the aluminium matrix whereas it becomes lower for non-FGM disc. However there is significant change is detected in the radial and tangential strain rates. The radial strain rate first decreases to a certain radius and here it becomes minimum but after that it again starts increasing. Figure 5.14 shows that the tangential strain rates are affected by the reinforcements. But the decreasing trend of strain rates remains same as shown by figure 5.10.

CHAPTER 6

CONCLUSIONS

1. From the present investigation, it is observed that the steady state creep in Al-SiC_p disc under mechanical loading condition, can be described in a better way by keeping the stress exponent value n=5 rather than n=3 or 8.
2. The result obtained from the present mathematical formulation confirms that the value of stress exponent plays an important role in the distribution of stresses and strains in the rotating FGM disc. The radial stress related to n=3 is highest whereas for n=8 is lowest over the entire disc.
3. Tangential cum effective stress results in the disc is also affected by varying the stress exponent but the influence is just the reverse at outer radius as compared to the inside radius.
4. It is also observed that the steady state creep rates are not affected much but the strain rates in FGM rotating disc are significantly diverge by changing the particle content size.
5. Changing the reinforcement volume also affects the creep results
6. The present study accomplishes that the distribution of strain rates both radial & tangential are significantly affected by variable stress exponent n, different particle content size*(P)* and varying reinforcement volume mixture.

FUTURE SCOPE OF THE STUDY

1. The current study is carried out at 623 K operating temperature. So the present investigation can be carried out at higher temperature than previously used.
2. Constant thickness is assumed in the study. It can be extended for variable thickness profiles also.
3. Reinforcement constant varied linearly in the present study from inner to outer radius, other variations can also be studied.

REFERENCES

1. **A. M. Wahl, G. O Sankey, M. J. Manjoine and E. Shoemaker**, "Creep Tests of Rotating Disks at Elevated Temperature and Comparison with Theory", *Journal of Applied Mechanics*, 21 **(1954)** 225–235.

2. **A.M. Zenkour,** "Stress Distribution in a Rotating Composite Structures of Functionally Graded Solid disks", *Journal of Materials Processing Technology,*209,**(2009)**, 3511–3517.

3. **A.M. Afsar, J. Go,** "Finite Element Analysis of Thermo elastic Field in a Rotating FGM circular Disk", *Applied Mathematical Modeling*, 34, **(2010)**, 3309-3320.

4. **D. Deepak, V. K. Gupta and A. K. Dham**, "Creep Modeling in Functionally Graded Rotating Disc of Variable Thickness" , *Journal of Mechanical Science and Technology,* 24 (11) **(2010)** 2221-2232.

5. **D Deepak, V.K. Gupta and A.K. Dham, "**Impact of Stress Exponent on Steady State Creep in a Rotating Composite Disc**",** *The Journal of Strain Analysis for Engineering Design***,** 44 **(2009)** 127-135.

6. **GurkanAltan and MuzafferTopcu**, "Thermo-Elastic Stress of a Metal-Matrix Composite Disc under Linearly-Increasing Temperature Loading by Analytical and FEM Analysis," *Advances in Engineering Software,* 41 **(2010)** 604–610.

7. **HasanCallioglu**, "Stress Analysis in a Functionally Graded Disc under Mechanical Loads and a Steady State Temperature Distribution", *Sadhana (*36), Part 1, **(2011)** 53–64.

8. **HasanCallioglu, NumanBehlulBektas andMetinSayer,** "Stress Analysis of Functionally Graded Rotating Discs: Analytical and Numerical Solutions", *Acta Mech. Sin,* 27(6) **(2011)** 950–955.

9. **J.N. Sharma, Dinkar Sharma and Sheo Kumar,** "Stress and Strain Analysis of Rotating FGM Thermo elastic Circular Disk by Using FEM", *International Journal of Pure Applied Mathematics*, 74, **(2012)**, 339-352.

10. **M. Bayat, B.B.Sahari, M. Saleem, Aidy Ali and S.V. Wong**, "Bending Analysis of a Functionally Graded Rotating Disk Based on the First Order Shear Deformation Theory", *Applied Mathematical Modeling,* 33 **(2009)** 4215–4230.

11. **M. Damircheli1 and M.Azadi,** "Temperature and Thickness Effects on Thermal and Mechanical Stresses of Rotating FG-Disks", *Journal of Mechanical Science and Technology,* 25 (3) **(2011)** 827-836.

12. **M. Rattan, N. Chamol and S. B. Singh**, "Creep Analysis of an Isotropic Functionally Graded Rotating Disc", *International Journal of Contemp. Math. Sciences*, **5**, **(2010)**, 419 – 431.

13. **NakiTutuncu and BeytullahTemel**, "A Novel Approach to Stress Analysis of Pressurized FGM Cylinders, Disks and Spheres", *Composite Structures,* 91 **(2009)** 385–390.

14. **R.K. Shukla,** "Creep Transition in a Thin Rotating Non-Homogeneous Disc", *Indian Journal of Pure Applied Mathematics,*27(5),**(1996)**, 487-498.

15. **S.B. Singh and S. Ray,** "Steady state Creep Behavior in an Isotropic Functionally Graded material rotating Disc of Al-SiC composite", *Metallurgical and Materials Transactions A*, 32A**,(2001)**, 1679-1685.

16. **S.B. Singh and S. Ray, "**Creep Analysis in an Isotropic FGM Rotating Disc of Al-SiC Composite", *Journal of Materials Processing Technology*, 143–144,**(2003)**, 616–622.

17. **S.B. Singh and S. Ray,** "Newly Proposed Yield Criterion for residual Stresses and Steady State Creep in an Anisotropy Composite Rotating Disc", *Journal of Materials Processing Technology,*143–144,**(2003)**, 623–628.

18. **S.B. Singh, "**One Parameter Model for Creep in a Whisker Reinforced Anisotropic Rotating Disc of Al-SiC_w Composite", *European Journal of Mechanics A/Solids,*27, **(2008),** 680-690.

19. **V.K. Gupta, S.B. Singh, H.N. Chandrawat and S. Ray,** "Steady State Creep and Material Parameters in a Rotating Disc of Al-SiC_p Composite", *European Journal of Mechanics A/Solids,*23, **(2004)**, 335-344.

20. **V.K. Gupta, S.B. Singh, H.N. Chandrawat and S. Ray**, "Creep Behavior of a Rotating Functionally Graded Composite Disc Operating under thermal Gradient", *Metallurgical and Materials Transactions A,*35A, **(2004)**, 1381-1391.

21. **V.K. Gupta, S.B. Singh, H.N. Chandrawat and S. Ray,** "Modeling of Creep Behavior of a Rotating Disc in the Presence of Both composition and Thermal Gradients", *Journal of Mechanical Science and Technology*, 127, **(2005)**, 97-105.

22. **Vandana Gupta and S.B. Singh,** "Creep Modeling in a Composite Rotating Disc with Thickness Variation in Presence of Residual Stress", *International Journal of Mathematics and Mathematical Sciences,* Vol. **2012**Article ID 924921.

23. **Xu-Long Peng and Xian-Fang Li,** "Thermal Stress in Rotating Functionally Graded Hollow Circular Disks", *Composite Structures,* 92 **(2010)** 1896–1904.

24. **Xu-Long Peng and Xian-Fang Li**, "Effects of Gradient on Stress Distribution in Rotating Functionally Graded Solid Disks", *Journal of Mechanical Science and Technology,* 26 (5) *(***2012)** 1483-1492.

25. **Ashby, M. F**. "Technology in the 1990 Advanced Materials and Predictive Design," *Philosophical Transactions* of *the Royal Society of London,* A322 **(1987)** 393-407.

26. **Autar K. Kaw,** "Mechanics of Composites Materials", CRC Press Boca Raton, New York, **(1997)**

27. **Bryan Harris, "**Engineering Composite Materials", *The Institute of Materials, London*, **(1999)**.

28. **Marc Meyers and KrishanChawla, "**Mechanical Behavior of Materials*", Cambridge University Press,* IInd Edition, **(2009)**.

29. **D.S.Bedi,** "Strength of Materials", *S. Chand & Company Ltd.*

30. **en.wikipedia.org/**wiki/Dislocation_creep

31. **engineering.dartmouth.edu/**defmech/chapter_2.htm.

32. **www.bss.phy.cam.ac.uk/**~amd3/teaching/A_Donald/Crystalline_solids_2.htm.

33. **www.abdmatrix.com**ATMindex.phpaction=downloadfile&filename=Introduction%20to%20Composite%20Materials.pdf&directory= (Pdfdownloaded on 17-10-2012)

34. **www.me.umn.edu/**labs/composites/Projects/Polymer%20Heat%20Exchanger/Creep%20description.pdf (Downloaded on 01-05-2013)